Genetic insight into zinc and antimicrobial toxicity uncovers a glycerol phosphate modification on streptococcal rhamnose polysaccharides

Rebecca J. Edgar[1], Vincent P. van Hensbergen[2, #], Alessandro Ruda[3, #], Andrew Turner[4], Pan Deng[5], Yoann Le Breton[6,7], Najib M. El-Sayed[6,7], Ashton T. Belew[6,7], Kevin S. McIver[6,7], Alistair G. McEwan[4], Andrew J. Morris[5], Gérard Lambeau[8], Mark J. Walker[4], Jeffrey S. Rush[1], Konstantin V. Korotkov[1], Göran Widmalm[3], Nina M. van Sorge[2,*], and Natalia Korotkova[1,*]

[1]Department of Molecular and Cellular Biochemistry, University of Kentucky, Lexington, Kentucky, USA

[2]Department of Medical Microbiology, University Medical Center Utrecht, Utrecht University, Utrecht, The Netherlands

[3]Department of Organic Chemistry, Arrhenius Laboratory, Stockholm University, Stockholm, Sweden

[4]Australian Infectious Diseases Research Centre and School of Chemistry and Molecular Biosciences, The University of Queensland, Brisbane, Australia

[5]Division of Cardiovascular Medicine and the Gill Heart Institute, University of Kentucky Lexington, Kentucky, USA

[6]Department of Cell Biology & Molecular Genetics and Maryland Pathogen Research Institute,

[7]Center for Bioinformatics and Computational Biology, University of Maryland, Maryland, USA

[8]Université Côte d'Azur (UCA), Centre National de la Recherche Scientifique (CNRS), Institut de Pharmacologie Moléculaire et Cellulaire (IPMC), Valbonne Sophia Antipolis, France

[#]These authors contributed equally to this work.

*Corresponding authors. Correspondence and request for materials should be addressed to N.K. (email: nkorotkova@uky.edu) and N.M.vS. (email: nsorge3@umcutrecht.nl).

Abstract

Phosphate-containing polyanionic glycopolymers, such as wall teichoic acid (WTA), play important roles in many fundamental aspects of bacterial physiology and infection biology. Interestingly, the cell walls of many streptococcal species express glycopolymers that are considered to be WTA homologues but surprisingly lack the characteristic and biologically-relevant anionic charge. The human pathogen Group A *Streptococcus* (GAS; *Streptococcus pyogenes*) expresses the species-defining Group A Carbohydrate (GAC), which consists of a polyrhamnose backbone with *N*-acetylglucosamine (GlcNAc) side-chains that are important for pathogenesis. We identified *gacH*, a gene of unknown function located in the GAC biosynthesis cluster, in two independent transposon library screens for its ability to confer resistance to zinc and susceptibility to the bactericidal enzyme human group IIA secreted phospholipase A_2 (hGIIA). To understand the underlying mechanism of these phenotypes, we expressed and crystallized the extracellular domain of GacH and demonstrate that it represents a new family of glycerol phosphate (GroP) transferases that is evolutionarily distinct from lipoteichoic acid synthase. Importantly, we demonstrate that GAC and also the homologous Serotype *C* Carbohydrate (SCC) from the dental pathogen *Streptococcus mutans* contain previously unidentified GroP modifications conferred by *gacH* and *sccH* products, respectively. NMR analysis of purified GAC revealed that approximately 30% of the GlcNAc side-chains of GAC are modified by GroP at the C6 hydroxyl group. In conclusion, our findings pinpoint a previously unrecognized structural modification of streptococcal cell wall polysaccharides that has important biological consequences, conferring negative charge to the bacterial cell wall. Furthermore, considering that GAC and homologous structures in other streptococcal pathogens are highly regarded targets for vaccine development, our discovery has implications for vaccine design.

Gram-positive bacteria are surrounded by a thick cell wall, which consists of a complex network of peptidoglycan with covalently attached glycopolymers. Cell wall glycopolymers comprise a large family of structurally diverse molecules, including wall teichoic acid (WTA), mycobacterial arabinogalactans and capsular polysaccharides[1-4]. From these, WTA is perhaps the most widespread and certainly the best-studied molecule. This polyanionic phosphate-rich glycopolymer is critical for functions such as cell division, antibiotic resistance, metal ion homeostasis, phage-mediated horizontal gene transfer and protection of bacteria from host defense peptides and antimicrobial enzymes [1,4]. As such, these structures and their biosynthetic pathways are attractive targets for therapeutic intervention, such as antibiotic development and vaccine design. Interestingly, many streptococci lack expression of classical WTA and instead express functionally homologous glycopolymers that are characterized by the presence of L-rhamnose (Rha), but are thought to lack the anionic charge due to the apparent absence of phosphate. These structures, referred to as Streptococcal Rhamnose Polysaccharides (SRPs), comprise about 40-60% of the mass of the bacterial cell wall [5], and are historically used for serological grouping of streptococci [6]. The glycopolymers of two human streptococcal pathogens, Group A *Streptococcus* (GAS; *Streptococcus pyogenes*) and *Streptococcus mutans*, share a characteristic [→3)α-Rha(1→2)α-Rha(1→] polyrhamnose backbone, but are distinguished based on their specific glycosyl side residues, i.e. *N*-acetyl-β-D-glucosamine (GlcNAc) at the C3 position of Rha [7-9] in GAS and α-glucose (Glc) at the C2 position of Rha in *S. mutans c* serotype [10]. These conserved glycopolymers, referred to as the Lancefield group A Carbohydrate (GAC) and Serotype *c* specific Carbohydrate (SCC), play significant roles in the cell physiology and pathogenesis of GAS and *S. mutans*, respectively. The SCC-defective mutants show aberrant cell morphology and division [11], increased susceptibility to certain cell wall targeting antibiotics [12], defects in biofilm formation [13] and reduced ability to induce infective endocarditis compared to the parental strain [14]. Biosynthesis of the rhamnan-backbone of GAC is essential for GAS viability [15,16]. Moreover, GAS mutants deficient in the GAC GlcNAc side-chain are viable but more susceptible to innate immune clearance by neutrophils and antimicrobial agents, resulting in significant loss of virulence in animal models of GAS infection [15,17]. Importantly for both pathogens, GAC and SCC have been evaluated as universal vaccine antigens. This is especially attractive since L-Rha, is absent in mammalian cells reducing risk of cross reactivity with host tissues. Indeed, immunization with GAC and SCC induces opsonophagocytic antibodies that enhance killing of GAS and *S. mutans* respectively[10,18,19]. In addition, the GAC has proven efficacy as vaccine antigen in mouse models [18,19].

The GAC and SCC biosynthetic pathways are encoded by 12-gene clusters [15,20], herein designated as *gacABCDEFGHIJKL* and *sccABCDEFGHMNPQ* (Fig. 1), respectively. The first five genes in both operons, together with *gacG*/*sccG*, are conserved in many streptococcal species and they participate in polyrhamnose backbone synthesis and transport [21]. In GAS, we have demonstrated that *gacI, gacJ, gacK* and *gacL* encode the machinery to generate and add the immunodominant GlcNAc side-chain to the polyrhamnose backbone [15,22]. In *S. mutans, sccM* and *sccN* are required for immunoreactivity with serotype *c*-specific antiserum suggesting a function for these genes in Glc side-chain attachment to the polyrhamnose backbone [23]. In addition to these streptococcal species, similar gene clusters are present in a wide variety of streptococcal, lactococcal and enterococcal species, although the corresponding glycopolymer structures have not been elucidated [20]. Within this wider collection of species, one of the conserved genes present in the SRP biosynthetic clusters encodes a homolog of lipoteichoic acid (LTA) synthase (LtaS)[24-26] and LTA primase, LtaP[27,28]. LtaS and LtaP are glycerol phosphate (GroP) transferases that polymerize long chains of LTA – a membrane-anchored anionic polymer consisting of a 1,2-polyglycerol-phosphate backbone linked to a glycolipid membrane anchor. The *sn*-glycerol-1-phosphate (*sn*-Gro-1P) head group of phosphatidylglycerol functions as the glycerolphosphate donor for polymer synthesis occurring on the extracellular side of the plasma membrane [29]. The biological function of these LtaS/LtaP homologues in the biosynthesis of SRP is currently unknown.

Recently, we employed the *Krmit* GAS transposon mutant library [16] and identified *gacI* and *gacH* as factors that confer sensitivity of GAS to human secreted group IIA phospholipase A2 (hGIIA) (https://www.biorxiv.org/content/early/2018/02/23/269779) [30], an important bactericidal protein of the innate immune defense against Gram-positive pathogens [31]. Complementary, it was the only valid hit when exposing the *Krmit* library to a lethal concentration of hGIIA. In addition, *gacH* was identified by a transposon mutant library screen in a search for GAS genes providing resistance to zinc toxicity. In pursuit of the underlying mechanisms for GacH-mediated hGIIA resistance and protection against zinc toxicity, we have characterized the function of GacH at the genetic, biochemical and structural level. We have detected a previously overlooked GroP modification on both GAC and SCC and demonstrate a function of GacH homologs in the transfer of GroP to SRP. More importantly, using NMR analysis we show that GroP is attached to the GlcNAc side chains of GAC at the C6 hydroxyl group. These new insights into the structure, biosynthesis and function of GAC and SCC justify a re-examination of the chemical structures of cell wall glycopolymers in other streptococci. Also

this structural insight is important for future vaccine development and provides a framework for investigation of the function of the GroP cell wall modification in bacteria.

Results

GacH is required for full hGIIA bactericidal activity against GAS and *S. mutans*. We previously identified *gacH* as part of a GAS transposon library screen against the bactericidal human group IIA secreted phospholipase A2 protein called hGIIA [30]. In addition to this susceptibility screen, we also exposed the Krmit library to a lethal concentration of recombinant hGIIA, with only 47 colonies recovered after exposure. Sequencing identified that 43% of the recovered mutants (20 out of 47) had a transposon insertion in *gacH*, and 26% in *M5005_Spy_1390* (12 out of 47) (Fig. 2a). *M5005_Spy_1390* was also identified in the initial susceptibility screen as an artifact due to biased transposon insertions [30] and therefore not followed up further. To validate our finding for *gacH*, we generated a *gacH* deletion mutant in a GAS clinical isolate of the globally-disseminated serotype M1T1 clone 5448, creating 5448Δ*gacH*, and complemented the mutant with *gacH* on an expression plasmid. Exposure of this strain set to a concentration range of hGIIA confirmed that deletion of *gacH* increased GAS resistance to hGIIA more than 10-fold, which was restored back to wild-type (WT) upon introduction of the *gacH*-complementation plasmid (Fig. 2b). The *gacH*-mediated hGIIA resistance was also observed in two different GAS backgrounds, 2221 (M1T1 GAS clone strain) and 5005 (clinical *covS* mutant isolate of M1T1 strain) (Supplementary Fig. 1), demonstrating that the effect is conserved across GAS strains of the M1T1 background and independent of CovRS status – a two-component system which regulates about 15% of the genes in GAS [32].

Since other streptococcal species possess a genetic homolog of *gacH*, we investigated whether the GacH-dependent hGIIA-resistance phenotype was conserved in different streptococci. To this end, we generated a deletion mutant of the *gacH* homolog *sccH* (previously known as *orf7* [23]) in serotype *c S. mutans* (SMU) strain Xc, creating SMUΔ*sccH*. Similar to GacH in GAS, deletion of *sccH* rendered *S. mutans* unsusceptible to the tested hGIIA concentrations (Fig. 2c), which was restored to WT level by expression of *sccH* on a plasmid. Interestingly however, heterologous expression of *gacH* in SMUΔ*sccH* did not restore the hGIIA resistance phenotype, suggesting that the enzymes might target different substrates. Taken together, our data indicate that deletion of GacH homologs renders streptococci more resistant to the bactericidal activity of hGIIA and GacH function is species-specific. Interestingly, lack of the GAC GlcNAc side chain, by deletion of *gacI*, also induces increased hGIIA resistance, which

is associated with reduced cell wall penetration of hGIIA [30]. These data suggest that similar to *gacI*, *gacH* might participate in tailoring modification of GAC.

GacH and SccH provide protection from zinc toxicity. Recent evidence indicates that neutrophils deploy zinc poisoning as an antimicrobial strategy against GAS during phagocytosis [33]. To resist Zn (II) toxicity, GAS expresses the zinc efflux system encoded by *czcD* [33]. The *Krmit* GAS transposon library [16] was screened to identify additional GAS genes that confer resistance to zinc poisoning (Supplementary Fig. 2, Supplementary Fig. 3). In addition to the expected importance of *czcD*, we also observed that *gacI* and *gacH* transposon insertions were significantly reduced in the library (P-value of <0.05) after growth with 10 μM Zn (II) compared to untreated controls, indicating that the gene products provide resistance against zinc toxicity (Fig. 3).

To confirm that *gacI* and *gacH* are required for GAS resistance to zinc, we grew 5448Δ*gacH* and 5448Δ*gacI* [15] on THY agar supplied with different concentrations of Zn (II) (Fig. 4). The growth of both mutants was significantly reduced in THY supplied with 1.25 mM Zn (II). Expression of full-length *gacH* in 5448Δ*gacH,* and *gacI* in 5448Δ*gacI* fully complemented the growth phenotypes of the mutants (Fig. 4). To investigate whether *gacH* homologs protect other streptococci against zinc toxicity we extended our experiments to *S. mutans*. Similar to the GAS *gacH* deletion mutant, SMUΔ*sccH* was more sensitive to Zn (II) in comparison to the parental strain and the phenotype can only be restored by *sccH* but not *gacH* (Supplementary Fig. 4). Hence, our results provide strong evidence that the unknown functions of GacH and SccH are important for protection of streptococci from Zn (II) toxicity.

Phylogenetic analysis of the GacH family of proteins. Taking into consideration the conserved function of GacH homologs in hGIIA activity and protection against zinc toxicity in GAS and *S. mutans* we examined the distribution of the GacH family of proteins in bacteria. Interestingly, with a few exceptions, GacH homologs were found predominantly in streptococcal species (Fig. 5). In addition, we compared the evolutionary relatedness of GacH with GroP transferase enzyme involved in biosynthesis of LTA, LtaS. LtaS is composed of an N-terminal domain with five transmembrane helices and a C-terminal extracellular catalytic domain [25-28]. GacH is predicted to contain 11 transmembrane segments in its N-terminal domain and a C-terminal extracellular domain (eGacH), which is likely to perform the enzymatic function. Based on just the extracellular domains of the proteins, GacH and LtaS-related proteins clustered into distinct clades based on phylogenetic analysis, suggesting that the proteins may fulfill different functions in bacteria (Fig. 5).

GacH structure. To test the hypothesis that GacH is a GroP transferase, the extracellular domain of GacH (eGacH) was expressed and purified from *E. coli* and its crystal structures were determined in apo form and in complex with GroP (PDB IDs 5U9Z and 6DGM) (Fig. 6). The apo- and GroP-containing eGacH structures belong to the different crystal forms with two molecules in the asymmetric unit. Analysis of the dimer interface and other crystal contacts revealed that the dimer interface has the largest surface of all the crystal contacts (1809 and 1894 $Å^2$ in the two crystal forms) that scored below the stable complex formation criteria, and recombinant eGacH behaves as a monomer in solution. However, this does not exclude a possibility of a dimer formation in the context of the full-length GacH. Interestingly, the topology of the dimer observed in the asymmetric unit of eGacH structure orients the active sites towards the membrane, poised to engage the potential substrate, phosphatidylglycerol. The structures of the apo- and GroP-bound eGacH monomers are very similar with root mean square deviation of ~0.3 Å for 380 superimposed $C\alpha$ atoms, as well as between the non-crystallographic copies. eGacH has an α/β core structure that is similar of the sulfatase protein family, with the closest similarity to LtaS [25,26] and LtaP [27] (Supplementary Table 1). The catalytic site of GacH contained a Mn^{2+} ion coordinated by residues E488, T530, D711 and H712, equivalent to residues E255, T300, D475 and H476 of *S. aureus* LtaS (Fig. 6d and 6e, Supplementary Fig. 5). The structure of GacH in complex with GroP revealed the position of the ligand in the active site with the phosphoryl group oriented towards Mn^{2+} ion, and coordinated by residues G529, T530 and H650 (Fig. 6d). The glycerol 2- and 3-hydroxyl groups form hydrogen bonds with side-chains of residues R589, H580 and N586. The positions of GroP and coordinating residues are similar in eGacH and *S. aureus* LtaS structures, for example, the glycerol moiety forms hydrogen bonds with residues H580 and R589 in GacH and equivalent residues H347 and R356 in *S. aureus* LtaS (Fig. 6d and 6e) [25]. The structure of GacH in complex with GroP is consistent with the idea that GacH catalyzes GroP transfer to a substrate, similarly to the structurally related LtaS and LtaP proteins [25,27].

GacH homologs decorate SRP with GroP. The genetic, bioinformatic and structural evidence presented in the preceding sections strongly suggest that *gacH* and *sccH* encode novel GroP transferases of unknown function in GAS and *S. mutans* (Supplementary Fig. 6). The presence of these genes in the GAC and SCC biosynthetic clusters implies that they may participate in polysaccharide synthesis in a previously undefined manner. To investigate the possibility that GacH and SccH function in the modification of the respective SRPs with GroP, we enzymatically released SRP from purified cell walls (free of LTA, lipids, proteins and nucleic acids) from GAS 5005, *S. mutans* WT, and corresponding *gacH* and *sccH* deletion strains by

treatment with peptidoglycan hydrolases (as described in Materials and Methods). Subsequently, we analyzed the enriched polysaccharide preparations for glycerol and phosphate. Hydrolysis with HCl (2 N HCl, 100°C, 1 hr) released a significant amount of glycerol from GAC and SCC isolated from WT bacterial strains (Fig. 7 and Supplementary Fig. 7). Furthermore, we detected high levels of inorganic phosphate after incubation of these acid-treated samples with alkaline phosphatase (Fig. 7 and Supplementary Fig. 7). Of note, the treatment of intact GAC and SCC with alkaline phosphatase alone did not release detectable levels of phosphate (Supplementary Fig. 7), indicating that the phosphoryl moiety is present as a phosphodiester, presumably as GroP. In contrast to WT GAC and SCC, the SRPs isolated from 5005Δ*gacH* and SMUΔ*sccH* contained a significantly reduced amount of GroP (Fig. 7). Genomic complementation of 5005Δ*gacH* phenotype by expression of *gacH* on the mutant chromosome (Fig. 7) restored the WT levels of GroP in GAC. Similarly, complementation of SMUΔ*sccH* with plasmid-expressed *sccH* restored GroP incorporation of the mutant to the level of the parental strain. In contrast but in accordance with our functional data, expression of GacH did not restore the GroP levels in SCC of SMUΔ*sccH* (Fig. 7). Importantly, analysis of the glycosyl composition of cell walls purified from the GAS and *S. mutans* strains demonstrated that the absence of GacH and SccH did not affect the Rha/GlcNAc and Rha/Glc ratios, respectively (Supplementary Fig. 8). Since the differences in GroP content for 5005Δ*gacH* and SMUΔ*sccH* were not due to changes in the composition of GAC and SCC, our results are consistent with a role for SccH and GacH in modification of SRPs by GroP.

Purification of GAC for structural studies. To prepare bacterial polysaccharide for more detailed analysis, GAC was released from isolated cell walls by peptidoglycan hydrolase treatment and partially purified by a combination of size exclusion chromatography and ion-exchange chromatography. Fractions from ion-exchange chromatography were analyzed for Rha and total phosphate. The majority of the rhamnose- and phosphate-containing material was bound to the ion-exchange column and eluted as a single coincident peak (Fig. 8). Similarly prepared GAC purified from 5005Δ*gacH* did not bind to the column (Supplementary Fig. 9). Interestingly, the GAC from 5005Δ*gacH* does appear to contain a small amount of phosphate, although its phosphate content is much lower than the GAC isolated from the WT strain. This data directly supports the conclusion that GAC is modified by the addition of GroP units donated by GacH.

Identification of the enantiomeric form of GroP associated with GAC. LTA is formed by the sequential addition of *sn*-Gro-1-P groups transferred by LtaS from the head group of the membrane lipid phosphatidylglycerol [34,35]. In contrast, the poly-GroP backbone of WTA consists

of *sn*-Gro-3-P repeats that are synthesized on the cytoplasmic surface of the plasma membrane from CDP-glycerol before export to the periplasm and attachment to cell wall [1]. Since GacH and SccH are LtaS homologs, it is possible that the incorporated GroP is derived from phosphatidylglycerol yielding *sn*-Gro-1-P residues. To test this hypothesis, GroP was liberated from purified GAC by alkaline hydrolysis and separated from the polysaccharide by size-exclusion chromatography (SEC). As explained in detail by Kennedy *et al*. [36] for GroP modifications of membrane derived oligosaccharides, if GAC is modified by *sn*-Gro-1-P, alkaline hydrolysis of the phosphodiester bond should result in the formation of two cyclic intermediate compounds, Gro-1-cyclic phosphate and Gro-2-cyclic phosphate which are unstable in alkali and are cleaved to a mixture of *sn*-Gro-1-P and *sn*-Gro-2-P [36]. If GAC were modified by *sn*-Gro-3-P, alkaline hydrolysis would yield a mixture of *sn*-Gro-3-P and *sn*-Gro-2-P [36]. A phosphodiester of *sn*-Gro-2-P would give a mixture of all three phosphates [36]. Following alkaline hydrolysis the bulk of the carbohydrate still elutes in the void volume of the SEC column (Supplementary Fig. 10). However, the phosphate-containing fractions corresponding to the hydrolyzed GroP now elute in the inclusion volume (Supplementary Fig. 11). The enantiomeric composition of the GroP preparation following alkaline hydrolysis was determined by a combination of LC-MS and enzymatically by testing if the products are substrates for glycerol-3-phosphate dehydrogenase (G3PD). LC-MS revealed the presence of two GroP isomers, of approximately equal proportions, with LC retention times and major high molecular weight ions consistent with standard *sn*-Gro-1-P and *sn*-Gro-2-P (Fig. 9, Supplementary Fig. 11). To resolve whether *sn*-Gro-3-P or *sn*-Gro-1-P is the substituent, the recovered GroP was characterized further by enzymatic analysis with G3PD, which is strictly specific for *sn*-Gro-3-P. Under reaction conditions in which 500 pmol of *sn*-Gro-3-P produced a robust activity, incubation with either 500 pmol of *sn*-Gro-1-P or 500 pmol of the unknown Gro-P, recovered following alkaline hydrolysis, resulted in negligible activity (Supplementary Fig. 12). When a mixture containing 500 pmol of standard *sn*-Gro-3-P, and an equal amount of either *sn*-Gro-1-P or the unknown mixture of Gro-P isomers were tested, 85.8% and 90.0% of the activity detected with 500 pmol *sn*-Gro-3-P, alone, was found, demonstrating that the negative result using the unknown mixture, by itself, was not due to the presence of some inhibitory compound. Taken together, our results indicate that GacH decorates GAC with *sn*-Gro-1-P, which is most probably derived from phosphatidylglycerol.

GlcNAc side chains are required for GroP modification in GAC. The observation that the SMUΔ*sccH* mutant could only be rescued from from Zn (II) toxicity and acquisition of hGIIA resistance by expression of the native *sccH*, suggested that the site of GroP attachment

to SRPs might involve the species-specific side chains (Glc vs. GlcNAc), rather than the identical polyrhamnose backbone. Consistent with this hypothesis, the glycerol and phosphate contents in the SRP isolated from two GlcNAc-deficient mutants, 5005Δ*gacL* and 5005Δ*gacI*[22] are similar to those in 5005Δ*gacH* (Fig. 7d).

NMR spectroscopy confirms the presence of GroP at the C6 hydroxyl group of GlcNAc side chains. To establish the chemical structure of GAC, the polysaccharide isolated as described above (Fig. 8) was employed for NMR analysis. ^{1}H and ^{13}C NMR spectra of GAC confirmed the presence of Rha and GlcNAc in a 1.7:1 ratio as determined by a chemical analysis of its sugar components. Although the material was heterogeneous, initial analysis revealed that it would be possible to analyze the purified GAC at different levels of detail. The major component identifiable at the highest level of intensity in a multiplicity-edited ^{1}H,^{13}C-HSQC NMR spectrum (Supplementary Fig. 13), which had been acquired by non-uniform sampling at the 25% level of coverage facilitating enhanced resolution to resolve spectral overlap [37], revealed the ^{1}H NMR chemical shifts, including a resonance from an *N*-acetyl group, in very good agreement with those determined for GAC containing a polyrhamnan backbone and an GlcNAc side-chain with the following structure →3)-α-L-Rha*p*-(1→2)[β-D-Glc*p*NAc-(1→3)]-α-L-Rha*p*-(1→ as its repeating unit (RU); [8] thence the $^{1}J_{HC}$-based correlations facilitated identification of the resonances of the proton-carrying ^{13}C nuclei.

An array of 2D NMR experiments including ^{1}H,^{1}H-TOCSY, ^{1}H,^{1}H-NOESY, ^{1}H,^{13}C-HMBC and ^{1}H,^{13}C-HSQC-TOCSY led to the ^{1}H and ^{13}C NMR chemical shift assignments (Supplementary Table 2) and confirmed the structure of the trisaccharide RU. A number of additional cross-peaks were visible at the second intensity level of the ^{1}H,^{13}C-HSQC spectrum, particularly in the spectral region of methylene groups, e.g. hydroxymethyl groups of hexopyranses [38]. Besides the resonances from the hydroxymethyl group of the β-D-Glc*p*NAc residue at δ_H 3.78 and 3.94 correlated with a signal at δ_C 61.8 three more ^{13}C signals together with corresponding ^{1}H resonances were present at δ_C 63.1, 65.4 and 67.3 (Figure 10a), readily identified from the multiplicity-editing applied in the experiment. In the ^{13}C NMR spectrum two resonances at δ_C 67.3 and 71.6 were conspicuous in that they were split by 5.6 and 7.6 Hz, respectively. A ^{13}C resonance observed as a doublet in this manner suggests scalar coupling to the NMR active nucleus ^{31}P [39] and acquisition of a ^{31}P NMR spectrum on GAC showed a prominent resonance at δ_P 1.2. The ^{1}H,^{1}H-TOCSY NMR spectrum at the second intensity level revealed chemical shift displacements in the region for anomeric resonances (Supplementary Fig. 14) and in the ^{1}H,^{13}C-HSQC-TOCSY spectrum two correlations from the anomeric proton resonance at δ_H ~4.76 were observed to δ_C 61.8 (C6 in β-D-Glc*p*NAc) and to δ_C 65.4 (Figure

10b). Employing a $^{1}H,^{31}P$-HMBC experiment revealed correlations to protons of the latter carbon-13 at δ_H 4.10 and 4.19 as well as to δ_H 3.91 and 3.96, the ^{13}C nucleus of which resonates at δ_C 67.3 (Figure 10c). Moreover, a $^{1}H,^{31}P$-hetero-TOCSY experiment showed in addition to the just described proton correlations further correlations to δ_H 3.59, 3.64 and 3.70 (Figure 10d). Using the arsenal of 2D NMR experiments the resonances at the second level deviating from the parent structure were assigned (Supplementary Table 2). Thus, the GAC is partially substituted by a GroP residue at O6 of the side-chain β-D-Glc*p*NAc residue; based on integration of the cross-peaks for the anomeric resonances in the $^{1}H,^{13}C$-HSQC NMR spectrum the GAC preparation carries GroP groups to ~30 % of the GlcNAc residues. To validate the above results a triple-resonance $^{1}H,^{13}C,^{31}P$ NMR experiment based on through-bond $^{1}J_{HC}$ as well as $^{2}J_{CP}$ and $^{3}J_{CP}$ correlations [40] was carried out. The 3D NMR experiment revealed the ^{1}H NMR chemical shifts of H5' and the two H6' protons of the β-D-Glc*p*NAc residue as well as the two H1' protons and H2' of the Gro residue all correlated to ^{13}C nuclei (Fig. 10e), the ^{13}C NMR chemical shifts of C5' and C6' of the β-D-Glc*p*NAc residue as well as C1' and C2' of the Gro residue all correlated to the ^{31}P nucleus (Fig. 10f), and the above protons correlated to the ^{31}P nucleus (Fig. 10g). Taking into considerations the GacH-mediated mechanism of GAC modification by GroP as well as the biochemical experiments carried out herein, the substituent at O6 of β-D-Glc*p*NAc is an *sn*-Gro-1-P group (Fig. 11).

Discussion

In Gram-positive bacteria, peptidoglycan-attached carbohydrate-based polymers have a high degree of structural diversity within and between species. However, one common theme of most glycopolymers is the presence of negatively charged groups in the repeating units [4]. For example, canonical and non-canonical WTAs [41-44] and Group B Antigen of *Streptococcus agalactiae* contain phosphodiester groups in the repeating units [45,46], peptidoglycan of *Bacillus subtilis* grown in phosphate limiting conditions is decorated by a teichuronic acid containing glucuronic acid [47,48], and secondary cell wall carbohydrates of *Bacillus anthracis* are modified by pyruvyl groups [49]. Cell envelopes of most Gram-positive bacteria contain another class of teichoic acids — LTA [50-54]. These anionic poly-GroP-based structures are attached to the cytoplasmic membrane with a glycolipid anchor [53,54]. Negatively charged groups within WTA and LTA have been implicated in the binding and trafficking of metal cations, maintenance of the proton gradient across the cytoplasmic membrane and retaining envelope proteins including cell division autolysins [26,55-62]. In bacteria lacking WTA such as the human pathogens GAS and *S. mutans*, it has been proposed that other polyanionic structures fulfill similar functions during the

bacterial cell cycle [63 20]. Previous detailed studies using immunochemical methods, composition and linkage analyses and NMR methods deduced chemical structures of peptidoglycan-attached SRPs from these bacteria [7,9,10,64-66] but all failed to detect the presence of anionic groups in these structures, except one overlooked study in which the presence of glycerol and phosphate in GAC has been detected [67]. However, it was proposed that this GroP is part of the phosphodiester linkage connecting GAC to the N-acetylmuramic acid of PG [67].

In this report, we demonstrate that SRPs of GAS and *S. mutans* are actually polyanionic glycopolymers through decoration with GroP. Our NMR and biochemical studies of GAC revealed that 30 % of the GlcNAc side-chains are modified with *sn*-Gro-1-P at the C6 hydroxyl group. Interestingly, a number of reports identified substantial concentrations of phosphate in other SRPs isolated from *Streptococcus sanguis*, *Streptococcus gallolyticus*, *Streptococcus dysgalactiae*, *Streptococcus sobrinus* serotype *d* and *S. mutans* serotype *f* [34,66,68,69]. These phosphate-rich polymers were either disregarded as a contamination with LTA [34], or further analyzed using ^{1}H NMR or ^{13}C NMR methods [8-10,65,66,70,71] that are not suitable for detection of phosphoryl moieties in polysaccharides.

We found that novel GroP transferase enzymes, GacH and its homolog SccH, are required for SRP modification by GroP in GAS and *S. mutans*, respectively. Moreover, the GacH homologs are present in the SRP biosynthetic loci of many streptococci suggesting that a large group of streptococcal species produce SRPs where glycosyl side chains are decorated with GroP. GacH is predicted to be an extracellular protein anchored in the cytoplasmic membrane. It belongs to the alkaline phosphatase superfamily of which two GroP transferases involved in LTA synthesis, LtaS and LtaP, have been biochemically and structurally characterized to date [25-28]. LtaP initiates LTA synthesis by transferring the first GroP subunit onto a glycolipid anchor [27,28]. LtaS catalyzes the polymerization of LTA by repeated addition of GroP subunits to the glycerol end of the growing chain [24,35]. In addition, our BLAST search using the GacH sequence as query indicates that GacH has significant homology to OpgB-like enzymes involved in GroP modification of the osmoregulated periplasmic glucans in Gram-negative bacteria [72]. LtaS, LtaP and OpgB are membrane proteins that use the membrane lipid phosphatidylglycerol as the GroP donor for the transfer reaction [72,73]. The LtaS and LtaP crystal structures reveal a similar structural architecture with a serine residue in the catalytic site coordinating Mn^{2+} [25-27]. In addition, the LtaS crystal structure contains a GroP molecule complexed in the active site suggesting a catalytic mechanism in which a threonine residue functions as a nucleophile in phosphatidylglycerol hydrolysis [25-27]. Our structural analysis of GacH in complex with GroP indicates that the enzyme uses the catalytic T530 residue to

participate in the formation of a GroP-enzyme intermediate. We have shown that the GroP in GAC is the *sn*-Gro-1-P enantiomer, strongly suggesting that it must be derived from phosphatidylglycerol. These observations suggest a catalytic mechanism in which GacH binds phosphatidylglycerol and T530 functions as a catalytic nucleophile to attack the GroP head group and cleave the phosphodiester bond. Diacylglycerol is released, leaving a covalent GroP-Thr intermediate. Next, the C6 hydroxyl group of the GAC GlcNAc target is deprotonated and then attacks the GroP-Thr enzyme, forming the GroP-GlcNAc product and returning the enzyme to the apo state.

Interestingly, GroP was previously detected in *Lactococcus lactis* IL1403 and UC509.9 cell wall polysaccharides [74,75] and *Streptococcus pneumoniae* type 11 and 18 capsular polysaccharides [76]. In the type 18A polysaccharide, the GroP substituent is *sn*-Gro-3-P [77], similar to the GroP repeating unit in WTA [1]. Genetic analyses of corresponding polysaccharide biosynthetic gene clusters revealed the presence of a CDP-glycerol synthetase gene [78], which catalyzes biosynthesis of GroP in WTA. Together, this suggests a mechanism in which the modification of these polysaccharides occurs in the cytosol before the export of the polymer to outside of the membrane.

In Gram-positive bacteria the tailoring modification of WTA and LTA with D-alanine provides resistance against cationic antimicrobial peptides and proteins including vancomycin, daptomycin, polymyxin B, cathelicidins, and sPLA2-IIA [79-84] and promotes Mg^{2+} ion scavenging [85]. It has been assumed that incorporation of positively charged D-alanine into teichoic acids leads to increased bacterial surface charge resulting in reduced initial binding of cationic antimicrobial peptides to the bacterial surface due to ionic repulsion [82,86].

Our study demonstrates that addition of the negatively charged GroP group to SRPs protects streptococci from zinc toxicity but also renders bacteria more sensitive to hGIIA activity. A large body of published evidence indicates that phagocytic cells utilize Zn (II) intoxication to suppress the intracellular survival of bacteria [87]. The mechanism of microbial susceptibility to Zn toxicity is mediated by extracellular competition of Zn (II) for Mn (II) transport and thereby mediating toxicity by impairing Mn^{2+} acquisition [88]. Accordingly, the phenotypes of our mutants deficient in the GroP modifications and the GlcNAc side chains could be explained either by “trapping” of Zn (II) in the WT cell wall as a consequence of zinc binding to negatively-charged GroP, or the increased Mn^{2+}-binding capacity of GroP-modified bacterial cell wall which has been proposed to act as the conduit for the trafficking of mono- and divalent cations to the membrane [59].

hGIIA is a 14 kDa highly cationic enzyme that catalyzes the hydrolysis of membrane glycerophospholipids at the *sn-2* ester bond, including phosphatidylglycerol [89-91], ultimately leading to bacterial death. Traversal of this bactericidal enzyme across the Gram-positive cell wall to reach plasma membrane is a multi-step process that is not well understood. It is clear however, that this process is charge dependent as the absence of positively-charged D-alanine modifications in LTA and WTA severely compromises *Staphylococcus aureus* survival when challenged with hGIIA [80,91] suggesting a role for this modification either in repulsing hGIIA from the cell surface or in modifying the permeability through the cell envelope. Similarly, the GacH/SscH-dependent GroP modifications on SRPs are required for hGIIA to exert its bactericidal effect against GAS and *S. mutans*, respectively. We have previously demonstrated that loss of the GlcNAc GAC side chain strongly hampers trafficking of hGIIA through the GAS cell wall, with a minor contribution of reduced hGIIA binding to the cell surface [30]. Since GroP-modifications were also lost in this mutant, we assume that the mechanisms of the hGIIA-dependent phenotype are similar in the *gacI* and *gacH* mutants.

The structural model of GAC has been proposed [92] in which GAC exists in a helix with polyrhamnose forming the core of the helix and the GlcNAc side-chains located on the periphery. We suggest that decoration of the side-chains with GroP changes the macromolecular structure of SRPs from helical or more collapsed to a more extended or stretched conformation as a result of charge-charge repulsion of phosphodiester anionic linkages. Collapsed GroP-deficient SRP structures would make membrane less accessible for small proteins such as hGIIA. In contrast, the expended GroP-modified SRPs might trap cationic small toxic cations more efficiently resulting in increased resistance to these molecules.

Another very important aspect of our study is the identification of a novel, potentially antigenic, epitope on the surface of streptococcal bacteria. GAS is a significant human pathogen, and is associated with numerous diseases ranging from minor skin and throat infections such as impetigo and pharyngitis to life-threatening invasive diseases such as scarlet fever, streptococcal toxic syndrome and rapidly progressing deep-tissue infections, necrotizing fasciitis (i.e. the “flesh eating disease), cellulitis and erysipelas [93]. GAS infections are also responsible for post-infectious autoimmune syndrome, rheumatic fever (RF) and its sequel, rheumatic heart disease (RHD) [93]. The invasive GAS infections are difficult to treat with antibiotics and a GAS vaccine is urgently needed to combat this neglected disease. GAC is a very attractive candidate for a universal GAS vaccine due to its conserved expression in all GAS serotypes and the absence of the constitutive component of GAC, Rha, in humans [18,19]. However, immunological mimicry between GlcNAc side chain and human heart muscle proteins

has been reported [94]. Moreover, anti-GlcNAc antibodies have been detected in the patients with RF and RHD [94]. It has therefore been proposed that the GAC GlcNAc side chain can elicit these cross-reactive antibodies relevant to the pathogenesis of RF and RHD [95-97]. Moreover, persistence of anti-GAS and anti-GlcNAc antibodies is a marker of poor prognosis in RHD [96,98]. These clinical associations and the lack of understanding of the pathogenesis of GAS post-infectious RHD have hampered progress in the development of GAC-based vaccines against GAS. However, the GAC GlcNAc decorated with GroP might be a feasible candidate for GAS vaccine development because modified GlcNAc represents a unique epitope, which is absent from human tissues. Thus, our study has implications for design of a safe and effective vaccine against this important human pathogen for which a vaccine is not yet available and provides a framework for structure-function investigations of cell wall modifications in streptococci.

Methods

Bacterial strains, growth conditions and media

All plasmids, strains and primers used in this study are listed in Supplementary Tables 3 and 4. Streptococcal strains used in this study were the M1-serotype GAS strains, 5448 [16], 2221 [99] and 5005 [99], and *c* serotype *S. mutans* Xc [100]. GAS and *S. mutans* strains were grown in Todd-Hewitt broth supplemented with 1% yeast extract (THY) without aeration at 37 °C. *S. mutans* strains were grown in Todd-Hewitt broth without yeast extract for hGIIA mediated killing experiments. *E. coli* strains were grown in Luria-Bertani (LB) medium or on LB agar plates at 37 °C. When required, antibiotics were included at the following concentrations: ampicillin at 100 μg/mL for *E. coli*; streptomycin at 100 μg/mL for *E. coli*; erythromycin (Erm) at 500 μg/mL for *E. coli* and 5 μg/mL for GAS and *S. mutans*; chloramphenicol (CAT) at 10 μg/mL for *E. coli* and 2 μg/mL for GAS and *S. mutans*; spectinomycin at 200 μg/mL for *E. coli*, 100 μg/mL for GAS and 500 μg/mL for *S. mutans*.

To identify GAS genes providing resistance against zinc toxicity, we used chemically defined medium mRPMI. This medium is based on the formulation of RPMI 1640 medium [101] which mirrors the amino acid composition of the van de Rijn and Kessler formulation [102]. This RPMI 1640 (without glucose) (Gibco) is supplemented with nucleobases guanine, adenine and uracil at a concentration of 25 μg/mL each, as well as D-glucose at a final concentration of 0.5% w/v and HEPES at 50 mM. Necessary vitamins for GAS growth are provided by 100X BME Vitamins (Sigma B6891). The final solution is pH 7.4 and capable of supporting GAS growth without additional supplements.

Genetic manipulations

DNA techniques: Plasmids were transformed into GAS and *S. mutans* by electroporation as described previously [103]. Chromosomal DNA was purified from GAS and *S. mutans* as described [104]. All constructs were confirmed by sequencing analysis (Eurofins MWG Operon).

Genetic manipulation of GAS 5005 and 2221: For construction of the 5005Δ*gacH* and 2221Δ*gacH* strains, 5005 chromosomal DNA was used as a template for amplification of two DNA fragments using two primers pairs: 5005-f/gacHdel-r and gacHdel-f/5005-r. Primer gacHdel-f is complementary to primer gacHdel-r. The two gel-purified PCR products containing complementary ends were mixed and amplified using a PCR overlap method [105] with primer pair 5005-f/5005-r to create the deletion of *gacH*. The PCR product was digested with BamHI and XhoI and ligated into BamHI/SalI-digested plasmid pBBL740. The integrational plasmid pBBL740 does not have a replication origin that is functional in GAS, so the plasmid can be maintained only by integrating into the GAS chromosome through homologous recombination. The plasmid was designated pBBL740Δ*gacH*. The resulting plasmid was transformed into 5005 and 2221, and CAT resistant colonies were selected on THY agar plates. Five randomly selected colonies, that had the first crossover, were grown in liquid THY without CAT for ≥5 serial passages. Several potential double crossover mutants were selected as previously described [106]. The deletion in each mutant was confirmed by PCR sequencing of the loci.

To construct the plasmid for *in cis* complementation of the 5005Δ*gacH* mutant, 5005 chromosomal DNA was used as a template for amplification of a wild-type copy of *gacH* using the primer pair 5005-f/5005-r. The PCR products were digested with *BamHI* and *XhoI*, and cloned in pBBL740 previously digested with the respective enzymes. The plasmid was designated pBBL740*gacH*. The plasmid was transformed into the 5005Δ*gacH* strain, and CAT resistant colonies were selected on THY agar plates. Double crossover mutants were selected as described above. Selected mutants were confirmed by PCR sequencing, yielding strain *5005ΔgacH:gacH*$^{+}$

Genetic manipulation of GAS 5448: For construction of the 5448Δ*gacH* strains, GAS 5448 chromosomal DNA was used to amplify up and downstream regions flanking *gacH* using the following primer pairs: 5448-f/5448CAT-r and 5448CAT-f/5448-r. Primers 5448CAT-f and 5448CAT-r contain 25 bp extensions complementary to the CAT resistance cassette. Up- and downstream were fused to the CAT cassette using 5448-f/5448-r, digested with XhoI and HindIII and ligated into XhoI/HindIII-digested plasmid pHY304, yielding plasmid pHY304Δ*gacH*. After transformation in electrocompetent GAS 5448, transformed colonies were selected in THY containing Erm at 30 °C. After confirmation by PCR, transformed colonies were shifted to the non-permissive temperature of 37 °C to allow plasmid integration. Serial passage at 30°C in the

absence of antibiotic enabled occurrence of double cross-over events, yielding 5448Δ*gacH*, which were identified by screening for Erm sensitivity and CAT resistance. Deletion of *gacH* was confirmed by PCR.

To complement 5448Δ*gacH*, we created an expression plasmid p*gacH1*. *GacH* was amplified from GAS 5448 chromosomal DNA using primer pair gacH-EcoRI-f/gacH-BglII-r, digested using EcoRI/BglII, and ligated into EcoRI/BglII-digested pDCerm. p*gacH1* was transformed into the electrocompetent 5448Δ*gacH* and selected for Erm resistance on THY agar plates. Transformation was confirmed by PCR, yielding strain *5448ΔgacH:*p*gacH*.

Genetic manipulation of S. mutans Xc. For construction of the *sccH* deletion mutant (SMUΔ*sccH*), *S. mutans* Xc chromosomal DNA was used to amplify up and downstream regions flanking using the following primer pairs: sccH-f/sccH-erm-r and sccH-erm-f /sccH-r. Primers sccH-erm-f and sccH-erm-r contain 25 bp extensions complementary to the Erm resistance cassette. Up and downstream PCR fragments were mixed with the Erm cassette and amplified as a single PCR fragment using primer pair sccH-f/sccH-r. The *sccH* knockout construct was transformed into *S. mutans* as described previously [11]. Erm resistant single colonies were picked and checked for deletion of *sccH*/integration of Erm cassette by PCR using primer pair: sccH-c-f/sccH-c-r. The resultant strain, SMUΔ*sccH*, was complemented with homologous *sccH* or heterologous GAS gacH using complementation plasmid p*SccH* and p*GacH*, respectively. *SccH* and *gacH* were amplified from *S. mutans Xc* and GAS 5448 chromosomal DNA, respectively, using primer pairs sccH-EcoRI-f/sccH-BglII-r and gacH-EcoRI-f/gacH-BglII-r. The PCR products were digested with EcoRI/BglII, and ligated into EcoRI/BglII-digested pDC123 vector, yielding p*sccH* and p*gacH2*. The plasmids were transformed into SMUΔ*sccH* as described [11]. CAT resistant single colonies were picked and checked for presence of p*sccH* or p*gacH2* by PCR, yielding strains SMUΔ*sccH:*p*sccH* and SMUΔ*sccH:*p*gacH*.

Construction of the plasmids for E. coli *expression of gacH:* To create a vector for expression of extracellular domain of GacH, the gene was amplified from 5005 chromosomal DNA using the primer pair gacH-NcoI-f and gacH-XhoI-r. The PCR product was digested with NcoI and XhoI, and ligated into NcoI/XhoI-digested pET-NT vector. The resultant plasmid, pETGacH, contained *gacH* fused at the N-terminus with a His-tag followed by a TEV protease recognition site.

Protein expression and purification

For expression and purification of eGacH, *E. coli* Rosetta (DE3) cells carrying the respective plasmid were grown to an OD_{600} of 0.4-0.6 and induced at 18 °C for approximately 16 hrs. The cells were lysed in 20 mM Tris-HCl pH 7.5, 300 mM NaCl with two passes through a

microfluidizer cell disrupter. The soluble fractions were purified by Ni-NTA chromatography with washes of 20 mM Tris-HCl pH 7.5, 300 mM NaCl and 20 mM Tris-HCl pH 7.5, 300 mM NaCl, 10mM imidazole, and elution with 20 mM Tris-HCl pH 7.5, 300 mM NaCl, 250 mM imidazole. The eluate was dialyzed into 20 mM Tris-HCl pH 7.5, 300 mM NaCl in the presence of TEV protease (1 mg per 20 mg of protein). The dialyzed sample was reapplied to a Ni-NTA column equilibrated in 20 mM Tris-HCl pH 7.5, 300 mM NaCl to remove the cleaved His-tag and any uncleaved protein from the sample. eGacH was further purified by size exclusion chromatography on a Superdex 200 column in 20 mM HEPES pH 7.5, 100 mM NaCl, with monitoring for protein elution at 280 nm. Fractions collected during elution from the column were analyzed for purity by SDS-PAGE and concentrated to approximately 10 mg/mL.

For expression of seleno-methionine labelled eGacH, *E. coli* Rosetta (DE3) carrying eGacH was grown in LB at 37 ºC until an optical density at 600 nm of approximately 0.5 was obtained. The bacteria were centrifuged and resuspended in M9 minimal media supplemented with seleno-methionine. After a significant increase in optical density, protein expression was induced with 0.25 mM IPTG, and the cultures were grown at 16 ºC for approximately 16 hrs. Seleno-methionine labeled eGacH was purified as described above.

Crystallization, data collection and structure solution

eGacH crystallization conditions were initially screened using the JCSG Suites I–IV screens (Qiagen) at a protein concentration of 9 mg mL^{-1} by hanging drop vapor diffusion method. Crystals of Se-Met-substituted eGacH were grown in 0.1 M HEPES pH 7.5, 10% PEG8000, 8% ethylene glycol. Crystals were transferred into crystallization solution supplemented with 20% ethylene glycol and flash frozen in liquid nitrogen. The data were collected at APS 22-ID at a wavelength of 0.9793 Å. Crystals of GroP•eGacH complex were obtained using crystallization solution containing 0.2 M calcium acetate, 0.1 M MES pH 6.0, 20% PEG8000. *sn*-glycerol-1-phosphate (Sigma) was mixed with eGacH at 10 mM prior to crystallization. Initial crystals of GroP•eGacH complex belonged to the same crystal form as apo GacH, however, crystals of different morphology grew epitaxially after several days. These crystals displayed better diffraction and were used for structure determination of GroP•eGacH complex. Crystals were cryoprotected in crystallization solution supplemented with 10 mM GroP and 20% ethylene glycol and vitrified in liquid nitrogen. The data were collected at SSRL BL9-2 at a wavelength of 0.97946 Å.

All data were processed and scaled using *XDS* and *XSCALE* [107]. The structure of eGacH was solved by Se single-wavelength anomalous diffraction method. Se atoms positions were determined using HySS module in *PHENIX* [108,109]. The structure was solved using AutoSol

wizard in *PHENIX* [110]. The model was completed using *Coot* [111] and refined using *phenix.refine* [112]. The final structure has two eGacH molecules in the asymmetric unit containing residues 444–822.

The structure of GroP•eGacH complex was solved by molecular replacement using *Phaser* [113] and the dimer of apo eGacH as a search model. The model was adjusted using *Coot* and refined using *phenix.refine*. Difference electron density corresponding to GroP molecules was readily identified after refinement. GroP molecules were modeled using *Coot*. The geometric restraints for GroP were generated using Grade Web Server (http://grade.globalphasing.org) (Global Phasing). The last several rounds of refinement were performed using 19 translation/libration/screw (TLS) groups, which were identified by *PHENIX* [114].

The structures were validated using *Coot*, MolProbity [115] and wwPDB Validation Service (https://validate.wwpdb.org) [116]. Statistics for data collection, refinement, and model quality are listed in Supplementary Table 5. The structure factors and coordinates were deposited to the Protein Data Bank with accession codes 5U9Z (apo eGacH) and 6DGM (GroP•eGacH complex). Structure figures were generated using PyMOL v1.8.0.3 [117].

Isolation of cell wall

Cell wall was isolated from exponential phase cultures (OD_{600}=0.8) by the SDS-boiling procedure as described for *S. pneumoniae* [118]. Purified cell wall samples were lyophilized and used for carbohydrate composition analysis, phosphate and glycerol assays. Cell wall isolated from GAS 5005 was used for purification of GAC for *sn*-glycerol-1-phosphate identification and NMR analysis.

GAC purification

GAC was released from the cell wall by sequential digestion with mutanolysin (Sigma Aldrich) and recombinant PlyC amidase [22], and partially purified by a combination of size exclusion and ion-exchange chromatography. Mutanolysin digests contained 5 mg/mL of cell wall suspension in 0.1 M sodium acetate, pH 5.5, 2 mM $CaCl_2$ and 5 U/ml mutanolysin. Following overnight incubation at 37 ºC, soluble polysaccharide was separated from the cell wall by centrifugation at 13,000 x g, 10 min. Acetone (-20 ºC) was added to a final concentration of 80% and the polysaccharide was allowed to precipitate overnight at -20 ºC. The precipitate was sedimented (5,000 x g, 20 min), dried briefly under a stream of nitrogen gas and redissolved in 0.1 M Tris-Cl, pH 7.4. PlyC (50 μg/mL) was added to the GAC sample and the reaction was incubated overnight at 37 ºC. Following PlyC digestion GAC was recovered by acetone precipitation, as described above, redissolved in a small volume of 0.2 N acetic acid and chromatographed on a

25 mL column of BioGel P-10 equilibrated in 0.2 N acetic acid. Fractions (1.5 mL) were collected and monitored for carbohydrate by a minor modification of the anthrone assay. Fractions containing GAC (eluting near the void volume of the column) were combined, concentrated by spin column centrifugation (3,000 MW cutoff filter) and desalted by several rounds of dilution/reconstitution with water. After desalting, GAC was loaded onto an 18 mL column of DEAE-Sephacel. The column was eluted with a 100 ml gradient of NaCl (0-1 M). Fractions were analyzed for carbohydrate by the anthrone assay and phosphate by the malachite green assay following digestion with 70% perchloric acid (see below). Fractions containing peaks of carbohydrate were combined, concentrated by spin column (3,000 MW cut off) and lyophilized.

Anthrone assay

Total carbohydrate content was determined by a minor modification of the anthrone procedure. Reactions containing 0.08 mL of aqueous sample and water were prepared in Safe-Lock 1.5 mL Eppendorf Tubes. Anthrone reagent (0.2% anthrone, by weight, dissolved in concentrated H_2SO_4) was rapidly added, mixed thoroughly, capped tightly and heated to 100 ºC, 10 min. The samples were cooled in water (room temperature) and the absorbance at 580 nm was recorded. GAC concentration was estimated using an L-Rha standard curve.

Phosphate assay

Approximately 1.5 mg of cell wall material isolated from GAS was dissolved in 400 μL H_2O and 8 μg/mL PlyC, and incubated at 37 ºC, rotating for approximately 16 hrs. Additional PlyC was added and incubated for a further 4-6 hrs. To liberate SCC from *S. mutans* cell wall, 1.5 mg of cell wall material isolated from *S. mutans* were incubated 24 h with 1.5 U/ml mutanolysin in 400 μL of 0.1 M sodium acetate, pH 5.5, 2 mM $CaCl_2$. The samples were incubated at 100 ºC for 20 mins and centrifuged for 5 mins at maximum speed in a table top centrifuge. The supernatant was transferred to a new micro-centrifuge tube and incubated with 2 N HCl at 100 ºC for 2 hrs. The samples were neutralized with NaOH, in the presence of 62.5 mM HEPES pH 7.5. To 100 μL of acid hydrolyzed sample, 2 μL of 1 U/μL alkaline phosphatase (Thermo Fisher) and 10 μL 10 x alkaline phosphatase buffer was added and incubated at 37 ºC, rotating, overnight. Released phosphate was measured using the Pi ColorLock Gold (Innova Biosciences) kit, according to the manufacturer's protocol.

During GAC purification on BioGel P-10 and DEAE-Sephacel total phosphate content was determined by the malachite green method following digestion with perchloric acid. Fractions containing 10 to 80 μL were heated to 110 ºC with 40 μL 70% perchloric acid (Fisher Scientific) in 13 x 100 borosilicate disposable culture tubes for 1 h. The reactions were diluted to

160 μL with water and 100 μL was transferred to a flat-bottom 96-well culture plate. Malachite Green reagent (0.2 mL) was added and the absorbance at 620 nm was read after 10 min at room temperature. Malachite Green reagent contained 1 vol 4.2% ammonium molybdate tetrahydrate (by weight) in 4 M HCl, 3 vol 0.045% malachite green (by weight) in water and 0.01% Tween 20. The reagent is filtered and can be stored at 4 ºC for some time prior to use.

Glycerol assay

Samples for glycerol measurement were prepared as described for the phosphate assay but were not digested with alkaline phosphatase. Instead glycerol concentration was measured using the Glycerol Colorimetric assay kit (Cayman Chemical) according to the manufacturer's protocol.

Carbohydrate composition analysis

Carbohydrate composition analysis was performed at the Complex Carbohydrate Research Center (Athens, GA) by combined gas chromatography/mass spectrometry (GC/MS) of the per-O-trimethylsilyl derivatives of the monosaccharide methyl glycosides produced from the sample by acidic methanolysis as described previously by [119].

Identification of the stereochemistry of the GroP moiety of GAC

The stereochemistry of the GroP moiety attached to GAC was determined by a chemo-enzymatic method following release of GroP by alkaline hydrolysis as described by Kennedy *et al.* [36] using the Amplite™ Fluorimetric Glycerol-3-Phosphate Assay Kit (AAT Bioquest, Sunnyvale, CA). GAC was released from cell wall by sequential digestion with mutanolysin hydrolase and PlyC amidase, and partially purified by size exclusion chromatography (SEC) on Bio Gel P10 and ion exchange chromatography on DEAE Sephacel, as described above. GroP was liberated from the GAC by alkaline hydrolysis (0.5 M NaOH, 100 ºC, 1 h), neutralized with acetic acid and recovered from the inclusion volume following SEC on Bio Gel P10. Column fractions containing GroP were identified by HPLC/mass spectrometry (LC-MS) and fractions containing GroP were combined, concentrated by rotary evaporation (30 ºC, under reduced pressure) and desalted on BioGel P2. Column fractions containing GroP were combined, lyophilized and analyzed with the Amplite™ Fluorimetric Glycerol-3-Phosphate Assay Kit based on the production of hydrogen peroxide in the Gro-3-P oxidase-mediated enzyme coupled reaction. Reactions were conducted at room temperature for 10 to 20 minutes in solid black 96 well plates in a total volume of 0.1 ml. Excitation was at 540 nm and fluorescence at 590 nm was measured.

The fractions containing GroP were analyzed by LC-MS using a Q-exactive mass spectrometer and an Ultimate 3000 ultra high performance liquid chromatography system

(Thermo Fisher Scientific, San Jose, CA). Chromatographic separation was achieved using a silica-based SeQuant ZIC-pHILIC columns (2.1 mm × 150 mm, 5 µm, Merck, Germany) with elution buffers consisting of (A) 20 mM $(NH_4)_2CO_3$ with 0.1% NH_4OH in H_2O and (B) acetonitrile. The column temperature was maintained at 40 °C, and the flow rate was set to 150 µl/min. Mass spectrometric detection was performed by electrospray ionization in negative ionization mode with source voltage maintained at 3.0 kV. The capillary temperature, sheath gas flow and auxiliary gas flow were set at 275 °C, 40 arb and 15 arb, respectively. Full-scan MS spectra (mass range m/z 75 to 1000) were acquired with resolution R = 70,000 and AGC target 1e6.

Identification of hGIIA-resistant GAS transposon mutants

The GAS M1T1 5448 *Krmit* transposon mutant library [16] was grown to mid-log phase (OD_{600} = 0.4). 1 x 10^5 CFU were subjected to 27.5 µg/mL recombinant hGIIA [120] in triplicate and incubated for 1 h at 37 °C. Samples were plated on THY agar plates supplemented with kanamycin. The position of the transposon insertion of resistant colonies was determined as described previously [121].

hGIIA susceptibility assay

HGIIA susceptibility experiments were performed as described previously [30]. In short, mid-log suspensions (OD_{600} = 0.4), of GAS and *S. mutans* were diluted 1,000 times in HEPES solution (20 mM HEPES, 2 mM Ca^{2+}, 1% BSA [pH 7.4]) and 10 µL was added to sterile round-bottom 96 well plates in triplicates. Recombinant hGIIA was serially diluted in HEPES solution and 10 µl aliquots were added to bacteria-containing wells. Samples were incubated for 2 hrs at 37 °C (for GAS without CO_2, for *S. mutans* with 5% CO_2), PBS was added and samples were 10-fold serially diluted for quantification on agar plates. Survival rate was calculated as Survival (% of inoculum) = (counted CFU * 100) / CFU count of original.

Determination of selective metal concentrations

The Zn(II) sensitive gene deletion mutant 5448Δ*czcD* [33] was used to find the target concentration of Zn(II). Briefly, colonies of strains 5448 WT and 5448Δ*czcD* were scraped from THY agar plates and resuspended in PBS. After washing in PBS, the strains were adjusted to OD_{600} =1. These cultures were used to inoculate freshly prepared mRPMI containing varying concentrations of Zn(II) to starting OD_{600} = 0.05 in a 96-well plate. Growth at 37°C was monitored at OD_{595} every 15 min using the BMG Fluostar plate reader.

Tn-seq library screen for Zn(II) sensitivity

The 5448 Tn-seq library at T_0 generation [16] were thawed, inoculated into 150 mL prewarmed THY broth containing 300 µg/mL kanamycin and grown at 37 °C for 6 hrs. After 6 hrs growth,

the culture (T_1) was centrifuged at 4,000 x *g* for 15 min at 4 °C and the pellet resuspended in 32.5 mL saline. Freshly prepared mRPMI or mRPMI containing 10 μM or 20 μM Zn(II) was inoculated with 500 μL culture into 39.5 mL media, creating a 1:20 fold inoculation. These T_2 cultures were then grown at 37 °C for exactly 6 hrs, at which point 2 mL of these cultures were inoculated again into 38 mL of freshly prepared mRPMI alone or mRPMI containing 10 μM or 20 μM Zn(II). The remaining 38 mL of T_2 culture was harvested by centrifugation at 4,000 x *g* for 10 min at 4 °C and pellets stored at -20 °C for later DNA extraction. Cultures were grown for a further 6 hrs, at which point T_3 cultures were harvested by centrifugation at 4,000 x *g* for 10 min at 4 °C and pellets stored at -20°C.

DNA extraction and digestion for sequencing analysis

GAS pellets were extracted using the MasterPure complete DNA and RNA purification kit (Epicentre) with added enzymatic digestion in 10 mM Tris pH 8 and 100 mg/mL lysozyme and 50 mg/mL hyaluronidase. DNA was then purified as per manufacturers directions. Following purification, 6 μg of the genomic DNA was digested with *Mme*I (NEB) in a total volume of 400 μL with S-adenosylmethionine at 50 μM for 2 hrs at 37 °C. After digestion, DNA was then dephosphorylated with calf intestinal phosphatase (NEB) for a further 1 h. Digested, dephosphorylated DNA was then purified by extraction with phenol chloroform.

Adapter ligation and sequence amplification

Sequencing adapters 501 to 508 and 701 to 704 were used in this experiment (Supplementary Table 6) to allow sample multiplexing during massively parallel sequencing. 25 μL of purified *Mme*I digested, dephosphorylated DNA was ligated with 2 pmols of the appropriate sequencing adaptor in a reaction with T4 DNA ligase (NEB) at 16°C overnight.

Sequences were prepared by PCR amplification with primers oKrmitTNseq2 and AdapterPCR (Supplemental Table 2) using Accuprime Pfx in a 100 μL total reaction with 8 μL of ligation and primers at 1 μM final concentration for 22 cycles with an annealing temperature of 55 °C. PCR products were concentrated and a product at 186 bp was purified by agarose gel electrophoresis using the Wizard DNA cleanup kit (Promega). Purity and yield of the sequences was assessed using the Bioanaylzer instrument (Agilent).

Drop test assays

Strains 5448 WT, 5448Δ*gacI*, 5448Δ*gacI::gacI*, 5448Δ*gacH*, 5448Δ*gacH*:p*gacH*, *S. mutans* WT, SMUΔ*sccH*, SMUΔ*sccH:*p*sccH* and SMUΔ*sccH:*p*gacH* were grown in THY to mid-exponential growth phase, adjusted to OD_{600} = 0.6 and serial diluted. 5 μL were spotted onto THY agar plates containing varying concentrations of Zn(II) ($ZnSO_4 \cdot 7H_2O$). Plates were incubated at 37 °C

overnight and photographed. Drop tests are representative of biological replicates performed on at least 3 separate occasions.

NMR spectroscopy

The NMR spectra were recorded on a Bruker AVANCE III 700 MHz equipped with a 5 mm TCI Z-Gradient Cryoprobe ($^{1}H/^{13}C/^{15}N$) and dual receivers and a Bruker AVANCE II 600 MHz spectrometer equipped with a 5 mm TXI inverse Z-Gradient $^{1}H/D-^{31}P/^{13}C$. The ^{1}H and ^{13}C NMR chemical shift assignments of the polysaccharide material were carried out in D_2O solution (99.96 %) at 323.2 K unless otherwise stated. Chemical shifts are reported in ppm using internal sodium 3-trimethylsilyl-(2,2,3,3-$^{2}H_4$)-propanoate (TSP, δ_H 0.00 ppm), external 1,4-dioxane in D_2O (δ_C 67.40 ppm) and 2 % H_3PO_4 in D_2O (δ_P 0.00 ppm) as reference. The $^{1}H,^{1}H$-TOCSY experiments (dipsi2ph) were recorded with mixing times of 10, 30, 60, 90 and 120 ms. The $^{1}H,^{1}H$-NOESY experiments [122] were collected with mixing times of 100 and 200 ms. A uniform and non-uniform sampling (50 and 25 % NUS) were used for the multiplicity-edited $^{1}H,^{13}C$-HSQC experiments [123] employing an echo/antiecho-TPPI gradient selection with and without decoupling during the acquisition. The 2D $^{1}H,^{13}C$-HSQC-TOCSY were acquired using MLEV17 for homonuclear Hartman-Hahn mixing, an echo/antiecho-TPPI gradient selection with decoupling during acquisition and mixing times of 20, 40, 80 and 120 ms. The 2D $^{1}H,^{31}P$-Hetero-TOCSY experiments [124] were collected using a DIPSI2 sequence with mixing times of 10, 20, 30, 50 and 80 ms. The 2D $^{1}H,^{31}P$-HMBC experiments were recorded using an echo/antiecho gradient selection and mixing times of 25, 50 and 90 ms. The 3D $^{1}H,^{13}C,^{31}P$ [40] spectra were obtained using echo/antiecho gradient selection and constant time in t_2 with a nominal value of $^{n}J_{CP}$ of 5 Hz and without multiplicity selection. The spectra were processed and analyzed using TopSpin 4.0.1 software (Bruker BioSpin).

Bioinformatics analysis

The TOPCONS (http://topcons.net/) [125] web server was employed to predict trans-membrane regions of GacH. Homology detection and structure prediction were performed by the HHpred server (https://toolkit.tuebingen.mpg.de/#/tools/hhpred) [126]. To construct the GacH phylogenetic tree the homologs of full-length GacH (M5005_Spy_0609) were retrieved using blastp with an E-value cutoff of $1e^{-70}$. In addition, sequences were filtered based on a minimal identity of 33%, similarity of 73%, and having 11 predicted transmembrane helixes. Of all species expressing *gacH* homologues, *ltaS* homologues were retrieved using blastp and GAS *ltaS* (M5005_Spy_0622) as reference. As representatives of the LtaS and LtaP clades, five sequences of Listeria were selected that express both enzymes [27]. All protein sequences were aligned using MUSCLE [127]. The phylogenetic tree was build using MEGA6 [128] and the Maximum

Likelihood method based on the JTT matrix-based model [128]. For the phylogenetic tree with the extracellular domains of GacH and LtaS homologues, extracellular domains were predicted using http://www.cbs.dtu.dk/services/TMHMM/.

Statistical analysis

Unless otherwise indicated, statistical analysis was carried out from at least three independent experiments. Quantitative data was analyzed using the paired Student's t-test. A 2-way ANOVA with Bonferroni multiple comparison test was used to compare multiple groups. A *p*-value equal to or less that 0.05 was considered statistically significant.

Acknowledgements

This work was supported by the Center of Biomedical Research Excellence (COBRE) Pilot Grant (to KVK, NK and JSR) supported by NIH grant P30GM110787 from the National Institute of General Medical Sciences, by NIH grant 1S10OD021753 to AJM. NMvS and V.P.v.H were supported by VIDI grant 91713303 from the Netherlands Organization for Scientific Research (NWO). GW was supported by grants from the Swedish Research Council (no. 2013-4859 and 2017-03703) and The Knut and Alice Wallenberg Foundation. GL was supported by grants from CNRS, ANR (grant MNaims ANR-17-CE17-0012-01) and FRM (SPF20150934219).

Carbohydrate composition analysis at the Complex Carbohydrate Research Center was supported by the Chemical Sciences, Geosciences and Biosciences Division, Office of Basic Energy Sciences, U.S. Department of Energy grant (DE-FG02-93ER20097) to Parastoo Azadi.

Author contributions

AR, PD, YLB, KSM, AGM, AJM, GL, MJW, JSR, KVK, GW, NMvS and NK designed the experiments. RJE, VPvH, AR, AT, JSR, KVK, GW and NK performed functional and biochemical experiments. AR and GW performed NMR analysis. PD and AJM performed MS analysis. VPvH and NK constructed plasmids and isolated mutants. RJE, VPvH, AR, PD, YLB, NES, ATB, KSM, AGM, AJM, GL, MJW, JSR, KVK, GW, NMvS and NK analyzed the data. RJE, KVK, GW, NMvS and NK wrote the manuscript. All authors reviewed the results and approved the final version of the manuscript.

Figures

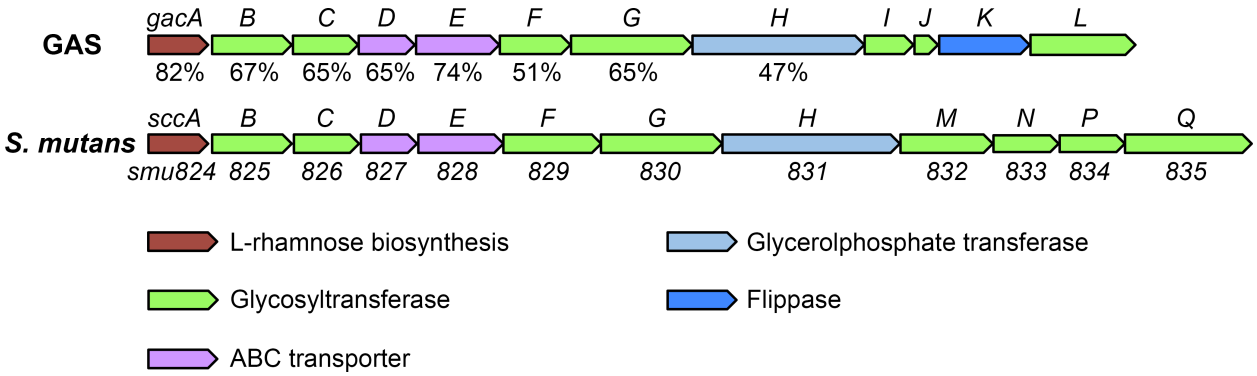

Fig. 1. Schematic representation of GAC and SCC biosynthetic gene clusters. Sequence identity (%) between homologous proteins is indicated. Sequences of *S. pyogenes* MGAS5005 and *S. mutans* UA159 were used for comparison.

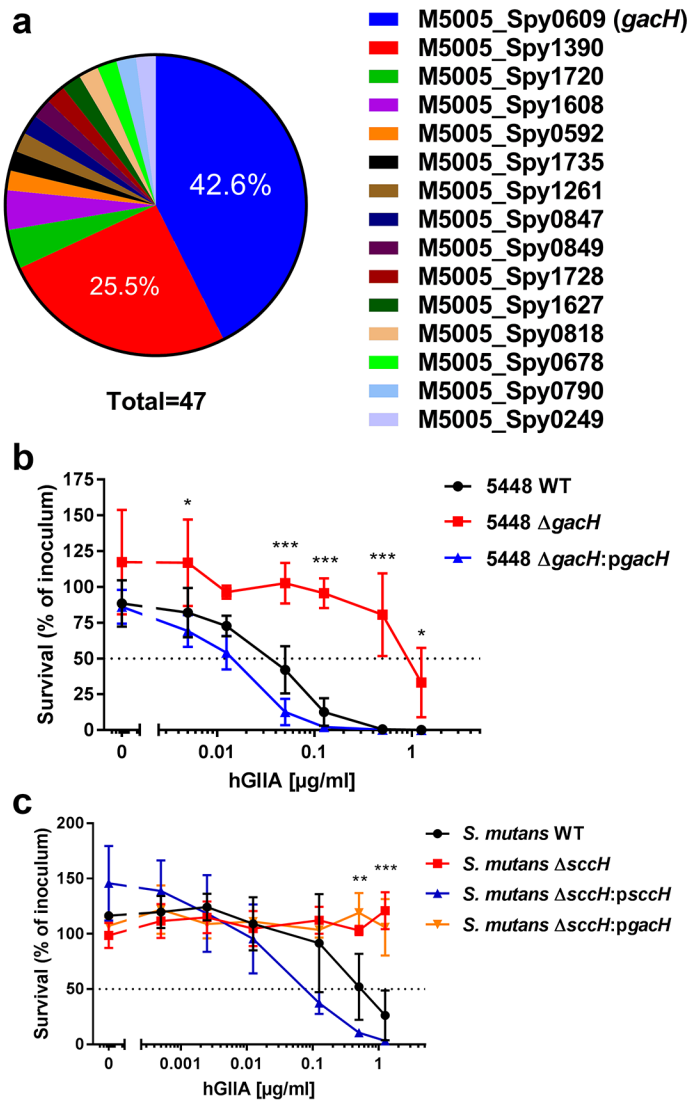

Fig. 2. *gacH* is identified in hGIIA-Tn-seq screen and its deletion confers resistance to hGIIA. a, Transposon gene location in 47 colonies after exposure of *Krmit* mutant transposon library to concentrations of hGIIA that are lethal to wild-type 5448 GAS. **b** and **c**, Deletion of *gacH* in GAS 5448 (**b**) and the *gacH*-homologous gene *sccH* in *S. mutans* (**c**) increases hGIIA resistance more than 10-fold. Data represent mean +/- SD of three independent experiments. *, $p > 0.05$; **, $p > 0.01$; ***, $p > 0.001$.

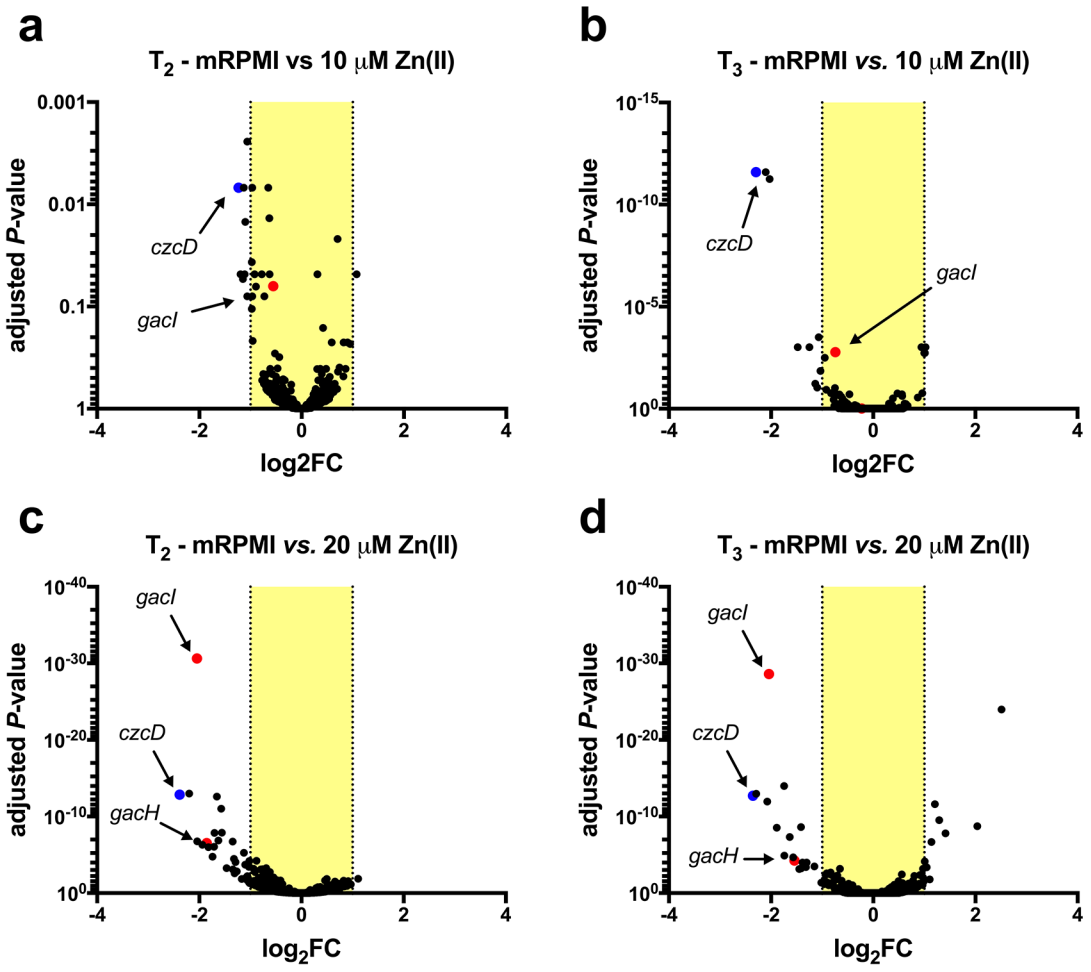

Fig. 3. Tn-seq volcano plots showing representation of *czcD*, *gacH* and *gacI* in screens. Log_2 fold-change in fitness was plotted against adjusted *P*-value from Tn-seq analysis. 10 μM Zn(II) at T_2 (**a**), 10 μM Zn(II) at T_3 (**b**), 20 μM Zn(II) at T_2 (**c**), 20 μM Zn(II) at T_3 (**d**).

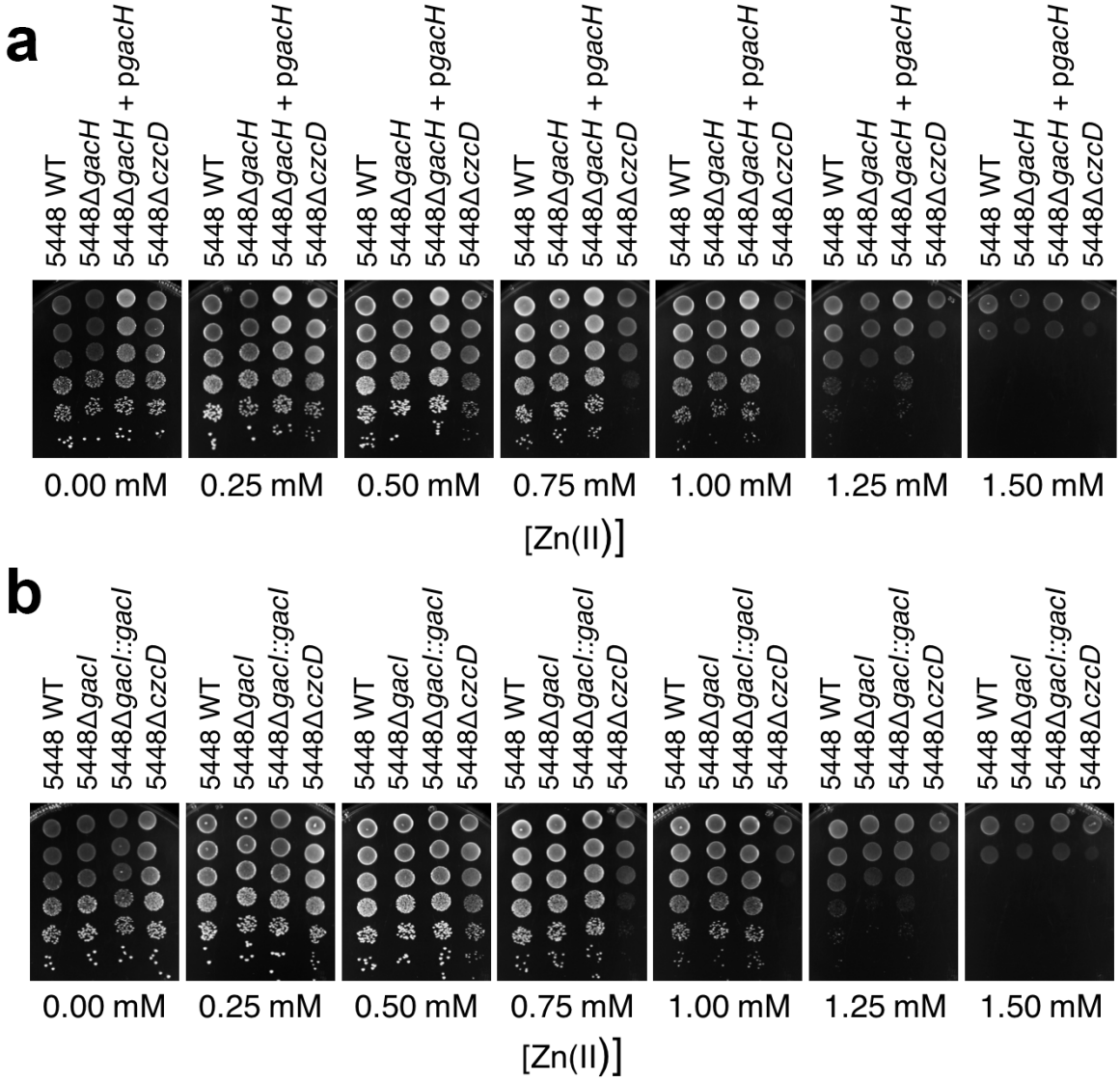

Fig. 4. Deletion of gacI and gacH renders GAS susceptible to Zn(II).

Zn(II) sensitivity as tested in drop assay using strains 5448 WT, 5448Δ*gacH*, 5448Δ*gacH:gacH* (**a**), 5448Δ*gacI*, 5448Δ*gacI:gacI* (**b**) with 5448Δ*czcD* included as a control. Strains were grown in THY to mid-exponential phase, adjusted to OD_{600} = 0.6, serial diluted and 5 µL spotted onto THY agar plates containing varying concentrations of Zn(II).

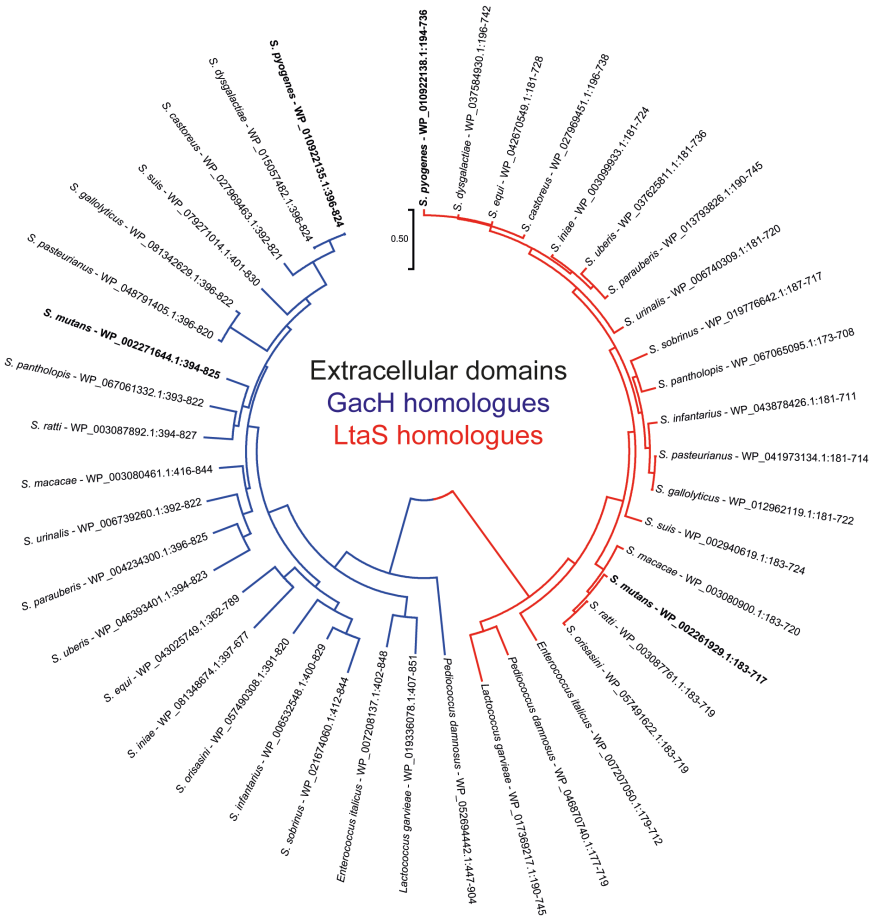

Fig. 5. GacH homologues from a distinct clade of GroP transferases. Phylogenetic analysis by Maximum Likelihood method of the predicted extracellular domains of GacH and LtaS enzymes. A phylogenetic tree was generated of the predicted extracellular domains of 21 GacH (blue) homologues and of the predicted extracellular domains of 21 LtaS (red) homologues from similar species. The GAS and SMU proteins analyzed in this study are indicated in bold. The phylogenetic tree is drawn to scale as indicated by the scale bar, with branch lengths measured in the number of substitutions per site.

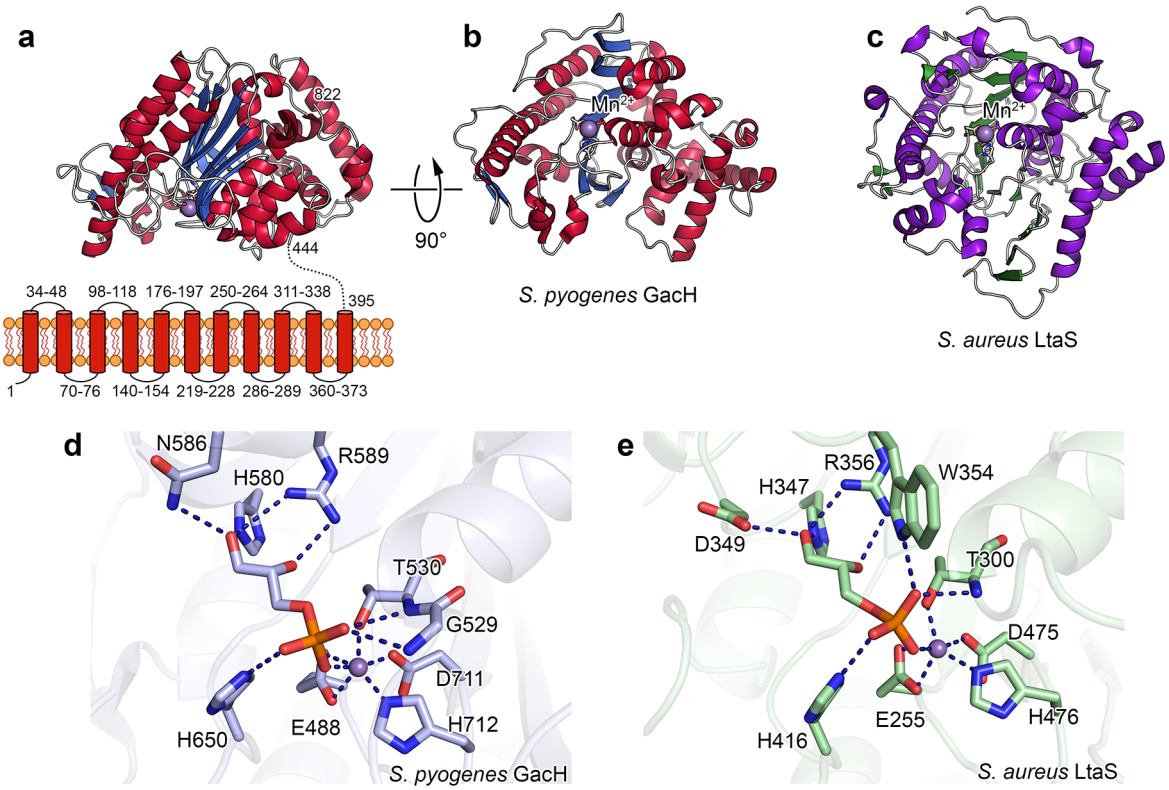

Fig. 6. Structure of GAS GacH. a, Predicted topology of GacH showing 11 transmembrane helices and structure of extracellular domain with the enzymatic active site oriented towards cell membrane. **b**, Structure of apo eGacH viewing at the active site with Mn^{2+} ion shown as a violet sphere. **c**, Structure of extracellular domain of *S. aureus* LtaS (PDB ID 2W5Q, [25]) shown in the same orientation as GacH. **d**, A close-up view of the active site GacH crystal structure in complex with *sn*-Gro-1-P. **e**, Comparison of the active site of LtaS (PDB ID 2W5T, [25]) with GroP in the active site.

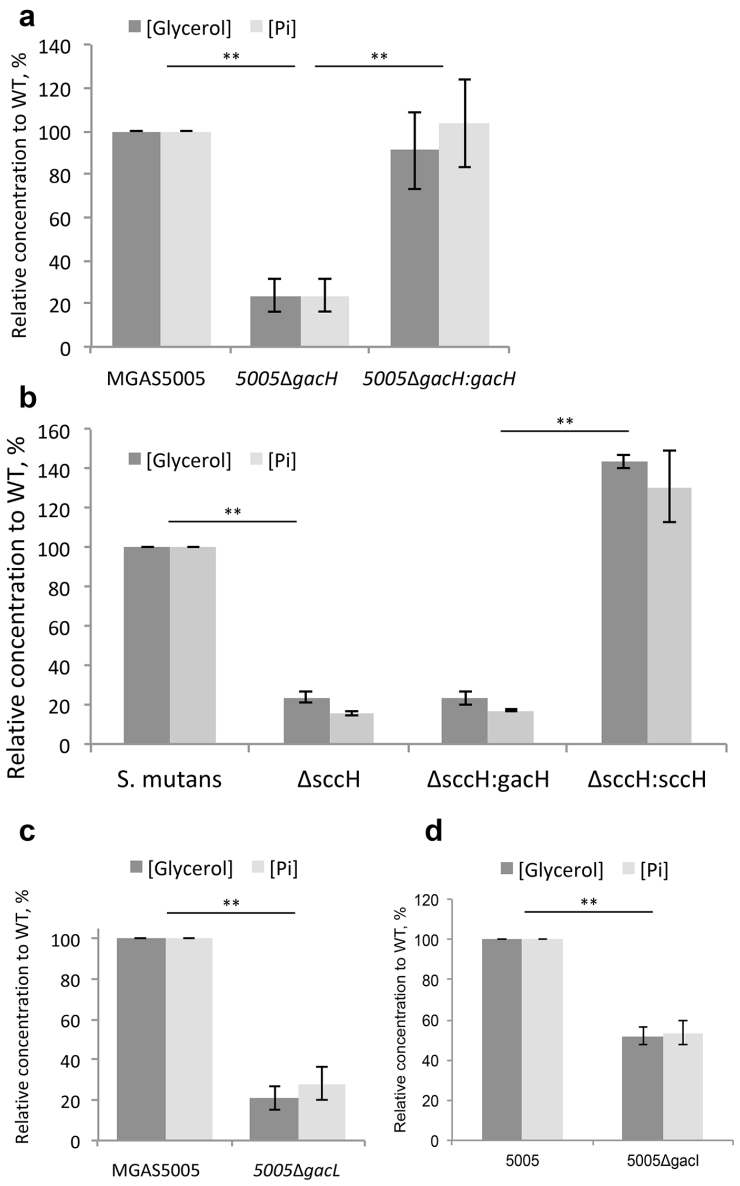

Fig. 7. Presence of glycerol and phosphate in SRPs from GAS and *S. mutans* depends on presence of side chain and GacH.

Analysis of glycerol and phosphate content in GAC and SCC isolated from the GAS and *S. mutans* strains, respectively. GAC and SCC were released from bacterial cell wall materials by PlyC and mutanolysin digestion, respectively, and subjected to acid hydrolysis as described in Methods. Phosphate was released from these samples by digestion with alkaline phosphatase and measured using the malachite green assay. Glycerol was measured using a colorimetric glycerol assay kit. The concentration of phosphate and glycerol is presented relative to the WT strain. Data are the mean ± standard deviation of three independent replicates. *, $p < 0.05$; **, $p < 0.01$ significance according to the Student's t-test.

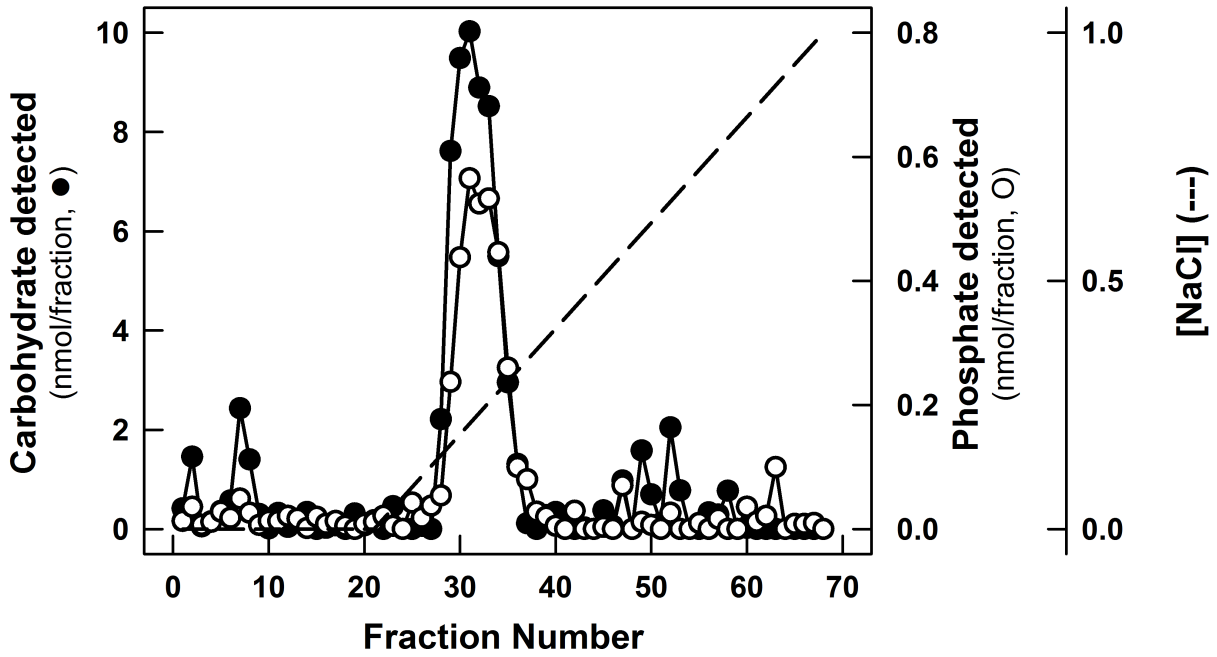

Fig. 8. DEAE-Sephacel elution profile of GAC. Isolated GAC was loaded onto an 18 mL column of DEAE-Sephacel. The column was eluted with a 100 ml gradient of NaCl (0-1 M). Fractions were analyzed for carbohydrate by anthrone assay and phosphate by malachite green assay.

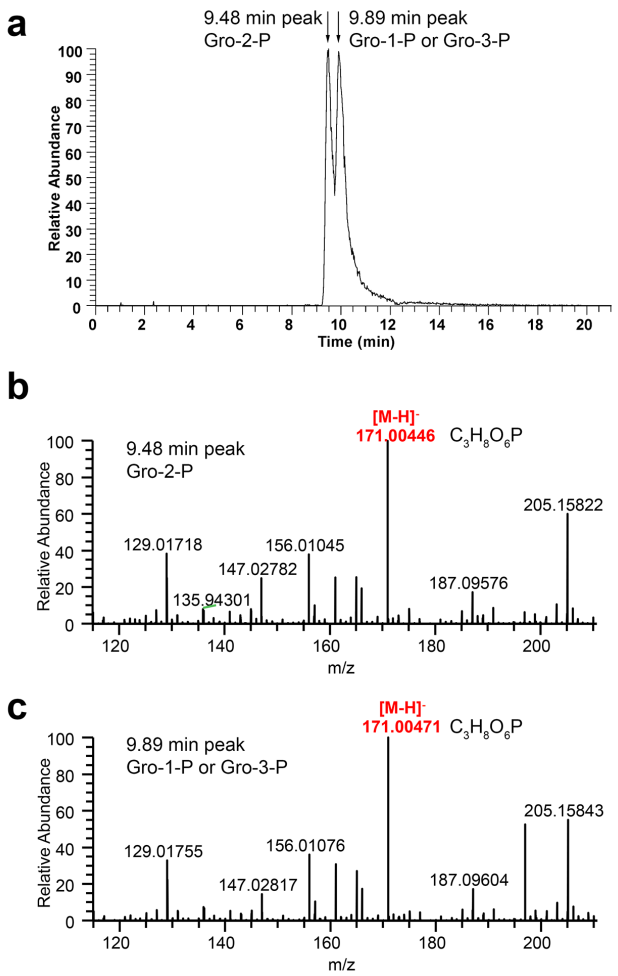

Fig. 9. Chromatography and Mass Spectrometry of the unknown GroPs recovered from GAS polysaccharide following alkaline hydrolysis. a, The elution positions of standard Gro 2P and Gro1 P/Gro 3P are indicated by the arrows. The Gro P isomers were resolved using an Ultimate 3000 ultra high performance liquid chromatography system (Thermo Fisher Scientific, San Jose, CA). Chromatographic separation was achieved with a silica-based SeQuant ZIC-pHILIC column (2.1 mm × 150 mm, 5 µm, Merck, Germany) with elution buffers consisting of (A) 20 mM $(NH_4)_2CO_3$ with 0.1% NH_4OH in H_2O and (B) acetonitrile. The column temperature was maintained at 40 °C, and the flow rate was set to 150 µl/min. **b**, Compounds were detected by mass spectrometry in negative ionization mode using a Q-exactive mass spectrometer with source voltage maintained at 3.0 kV. The capillary temperature, sheath gas flow and auxiliary gas flow were set at 275 °C, 40 arb and 15 arb, respectively. Full-scan MS spectra (mass range m/z 75 to 1000) were acquired with resolution R = 70,000 and AGC target 1e6. LC-high resolution mass spectrometry analysis identifies two extracted ion chromatogram peaks for the molecular glycerol phosphate ion *m/z* 171.004 ($[M-H]^-$), which eluted at 9.48 and 9.89 min. Based on the accurate mass and retention times, these two peaks were assigned as Gro2P and Gro1P/3P respectively by comparison with authentic chemical standards.

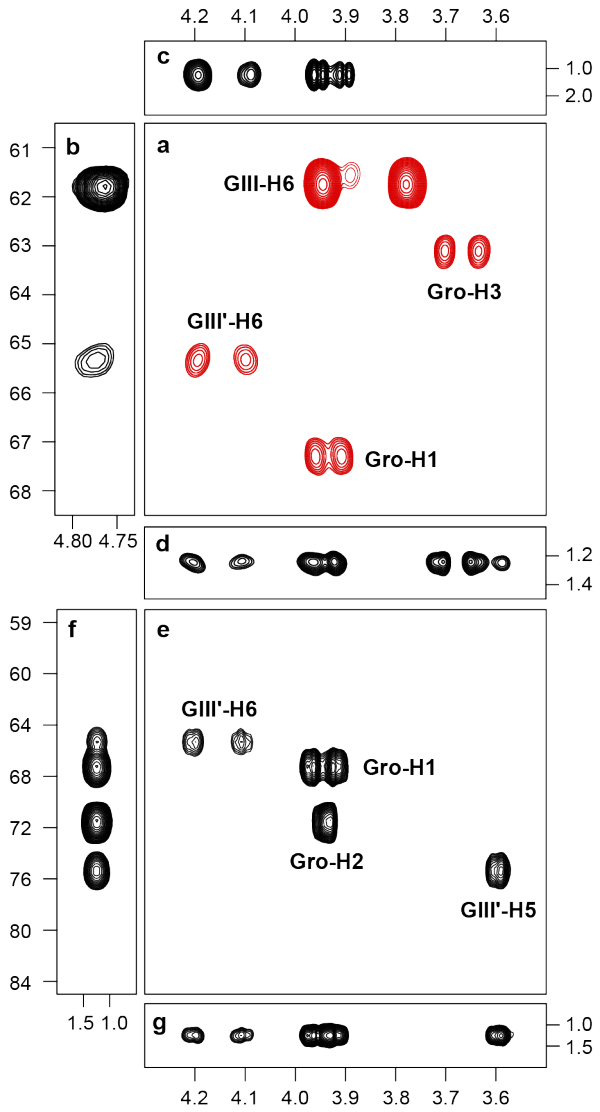

Fig. 10. NMR analysis confirms presence of GroP on GAC GlcNAc C6 hydroxyl group.

Selected regions of NMR spectra of the GAC polysaccharide. (**a**) Multiplicity-edited $^{1}H,^{13}C$-HSQC in which methylene groups have opposite phase and are shown in red color, (**b**) $^{1}H,^{13}C$-HSQC-TOCSY with an isotropic mixing time of 120 ms, (**c**) $^{1}H,^{13}C$-HMBC with a mixing time of 90 ms (**d**) $^{1}H,^{31}P$-hetero-TOCSY with an isotropic mixing time of 80 ms, (**e**) $^{1}H,^{13}C$-plane (**f**) $^{13}C,^{31}P$-plane using a nominal $^{n}J_{CP}$ value of 5 Hz and (**g**) $^{1}H,^{31}P$-plane of a through-bond 3D $^{1}H,^{13}C,^{13}P$ NMR experiment. Cross-peaks are annotated as GIII corresponding to the GlcNAc residue, GIII' being the phosphoglycerol-substituted GlcNAc residue and Gro as the glycerol residue. NMR chemical shifts of ^{1}H (horizontal axis),^{13}C (left axis) and ^{31}P (right axis) are given in ppm.

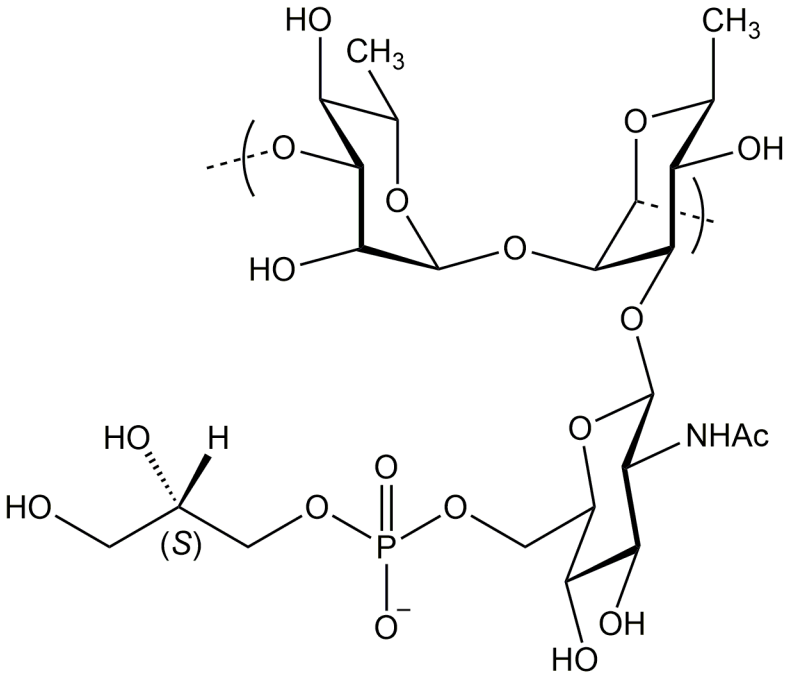

Fig. 11. Schematic structure of the redefined GAC repeating unit consisting of →3)-α-L-Rha*p*-(1→2)[β-D-Glc*p*NAc6*P*(*S*)Gro-(1→3)]-α-L-Rha*p*-(1→.

References

1 Brown, S., Santa Maria, J. P., Jr. & Walker, S. Wall teichoic acids of gram-positive bacteria. *Annu Rev Microbiol* **67**, 313-336, doi:10.1146/annurev-micro-092412-155620 (2013).

2 Chapot-Chartier, M. P. & Kulakauskas, S. Cell wall structure and function in lactic acid bacteria. *Microbial cell factories* **13 Suppl 1**, S9, doi:10.1186/1475-2859-13-S1-S9 (2014).

3 Jankute, M., Cox, J. A., Harrison, J. & Besra, G. S. Assembly of the Mycobacterial Cell Wall. *Annu Rev Microbiol* **69**, 405-423, doi:10.1146/annurev-micro-091014-104121 (2015).

4 Weidenmaier, C. & Peschel, A. Teichoic acids and related cell-wall glycopolymers in Gram-positive physiology and host interactions. *Nature reviews. Microbiology* **6**, 276-287, doi:10.1038/nrmicro1861 (2008).

5 McCarty, M. The lysis of group A hemolytic streptococci by extracellular enzymes of Streptomyces albus. II. Nature of the cellular substrate attacked by the lytic enzymes. *J Exp Med* **96**, 569-580 (1952).

6 Lancefield, R. C. A Serological Differentiation of Human and Other Groups of Hemolytic Streptococci. *J Exp Med* **57**, 571-595 (1933).

7 Coligan, J. E., Kindt, T. J. & Krause, R. M. Structure of the streptococcal groups A, A-variant and C carbohydrates. *Immunochemistry* **15**, 755-760 (1978).

8 Huang, D. H., Rama Krishna, N. & Pritchard, D. G. Characterization of the group A streptococcal polysaccharide by two-dimensional 1H-nuclear-magnetic-resonance spectroscopy. *Carbohydrate research* **155**, 193-199 (1986).

9 Pritchard, D. G., Coligan, J. E., Geckle, J. M. & Evanochko, W. T. High-resolution 1H- and 13C-n.m.r. spectra of the group A-variant streptococcal polysaccharide. *Carbohydrate research* **110**, 315-319 (1982).

10 St Michael, F. *et al.* Investigating the candidacy of the serotype specific rhamnan polysaccharide based glycoconjugates to prevent disease caused by the dental pathogen Streptococcus mutans. *Glycoconjugate journal*, doi:10.1007/s10719-017-9798-z (2017).

11 van der Beek, S. L. *et al.* GacA is essential for Group A Streptococcus and defines a new class of monomeric dTDP-4-dehydrorhamnose reductases (RmlD). *Mol Microbiol* **98**, 946-962, doi:10.1111/mmi.13169 (2015).

12 Tsuda, H., Yamashita, Y., Shibata, Y., Nakano, Y. & Koga, T. Genes involved in bacitracin resistance in Streptococcus mutans. *Antimicrob Agents Chemother* **46**, 3756-3764 (2002).

13 De, A. *et al.* Deficiency of RgpG Causes Major Defects in Cell Division and Biofilm Formation, and Deficiency of LCP proteins Leads to Accumulation of Cell Wall Antigens in Culture Medium by Streptococcus mutans. *Appl Environ Microbiol*, doi:10.1128/AEM.00928-17 (2017).

14 Nagata, E. *et al.* Serotype-specific polysaccharide of Streptococcus mutans contributes to infectivity in endocarditis. *Oral microbiology and immunology* **21**, 420-423, doi:10.1111/j.1399-302X.2006.00317.x (2006).

15 van Sorge, N. M. *et al.* The classical lancefield antigen of group a Streptococcus is a virulence determinant with implications for vaccine design. *Cell host & microbe* **15**, 729-740, doi:10.1016/j.chom.2014.05.009 (2014).

16 Le Breton, Y. *et al.* Essential Genes in the Core Genome of the Human Pathogen Streptococcus pyogenes. *Scientific reports* **5**, 9838, doi:10.1038/srep09838 (2015).

17 Henningham, A. *et al.* Virulence Role of the GlcNAc Side Chain of the Lancefield Cell Wall Carbohydrate Antigen in Non-M1-Serotype Group A Streptococcus. *MBio* **9**, doi:10.1128/mBio.02294-17 (2018).

18 Kabanova, A. *et al.* Evaluation of a Group A Streptococcus synthetic oligosaccharide as vaccine candidate. *Vaccine* **29**, 104-114, doi:10.1016/j.vaccine.2010.09.018 (2010).
19 Sabharwal, H. *et al.* Group A streptococcus (GAS) carbohydrate as an immunogen for protection against GAS infection. *J Infect Dis* **193**, 129-135, doi:10.1086/498618 (2006).
20 Mistou, M. Y., Sutcliffe, I. C. & van Sorge, N. M. Bacterial glycobiology: rhamnose-containing cell wall polysaccharides in Gram-positive bacteria. *FEMS Microbiol Rev* **40**, 464-479, doi:10.1093/femsre/fuw006 (2016).
21 Shibata, Y., Yamashita, Y., Ozaki, K., Nakano, Y. & Koga, T. Expression and characterization of streptococcal rgp genes required for rhamnan synthesis in Escherichia coli. *Infect Immun* **70**, 2891-2898 (2002).
22 Rush, J. S. *et al.* The molecular mechanism of N-acetylglucosamine side-chain attachment to the Lancefield group A Carbohydrate in Streptococcus pyogenes. *J Biol Chem*, doi:10.1074/jbc.M117.815910 (2017).
23 Ozaki, K. *et al.* A novel mechanism for glucose side-chain formation in rhamnose-glucose polysaccharide synthesis. *FEBS Lett* **532**, 159-163 (2002).
24 Grundling, A. & Schneewind, O. Synthesis of glycerol phosphate lipoteichoic acid in Staphylococcus aureus. *Proc Natl Acad Sci U S A* **104**, 8478-8483, doi:10.1073/pnas.0701821104 (2007).
25 Lu, D. *et al.* Structure-based mechanism of lipoteichoic acid synthesis by Staphylococcus aureus LtaS. *Proc Natl Acad Sci U S A* **106**, 1584-1589, doi:10.1073/pnas.0809020106 (2009).
26 Schirner, K., Marles-Wright, J., Lewis, R. J. & Errington, J. Distinct and essential morphogenic functions for wall- and lipo-teichoic acids in Bacillus subtilis. *EMBO J* **28**, 830-842, doi:10.1038/emboj.2009.25 (2009).
27 Campeotto, I. *et al.* Structural and mechanistic insight into the Listeria monocytogenes two-enzyme lipoteichoic acid synthesis system. *J Biol Chem* **289**, 28054-28069, doi:10.1074/jbc.M114.590570 (2014).
28 Webb, A. J., Karatsa-Dodgson, M. & Grundling, A. Two-enzyme systems for glycolipid and polyglycerolphosphate lipoteichoic acid synthesis in Listeria monocytogenes. *Mol Microbiol* **74**, 299-314, doi:10.1111/j.1365-2958.2009.06829.x (2009).
29 Fischer, W., Nakano, M., Laine, R. A. & Bohrer, W. On the relationship between glycerophosphoglycolipids and lipoteichoic acids in Gram-positive bacteria. I. The occurrence of phosphoglycolipids. *Biochim Biophys Acta* **528**, 288-297 (1978).
30 van Hensbergen, V. P. *et al.* Streptococcal Lancefield polysaccharides are critical cell wall determinants for human group IIA secreted phospholipase A2 to exert its bactericidal effects. *bioRxiv*, doi:https://doi.org/10.1101/269779 (2018).
31 Weiss, J. P. Molecular determinants of bacterial sensitivity and resistance to mammalian Group IIA phospholipase A2. *Biochim Biophys Acta* **1848**, 3072-3077, doi:10.1016/j.bbamem.2015.05.018 (2015).
32 Graham, M. R. *et al.* Virulence control in group A Streptococcus by a two-component gene regulatory system: global expression profiling and in vivo infection modeling. *Proceedings of the National Academy of Sciences of the United States of America* **99**, 13855-13860, doi:10.1073/pnas.202353699 (2002).
33 Ong, C. L., Gillen, C. M., Barnett, T. C., Walker, M. J. & McEwan, A. G. An antimicrobial role for zinc in innate immune defense against group A streptococcus. *J Infect Dis* **209**, 1500-1508, doi:10.1093/infdis/jiu053 (2014).
34 Emdur, L. I., Saralkar, C., McHugh, J. G. & Chiu, T. H. Glycerolphosphate-containing cell wall polysaccharides from Streptococcus sanguis. *J Bacteriol* **120**, 724-732 (1974).

35 Fischer, W., Laine, R. A. & Nakano, M. On the relationship between glycerophosphoglycolipids and lipoteichoic acids in Gram-positive bacteria. II. Structures of glycerophosphoglycolipids. *Biochim Biophys Acta* **528**, 298-308 (1978).
36 Kennedy, E. P., Rumley, M. K., Schulman, H. & Van Golde, L. M. Identification of sn-glycero-1-phosphate and phosphoethanolamine residues linked to the membrane-derived Oligosaccharides of Escherichia coli. *J Biol Chem* **251**, 4208-4213 (1976).
37 Orekhov, V. Y. & Jaravine, V. A. Analysis of non-uniformly sampled spectra with multi-dimensional decomposition. *Progress in nuclear magnetic resonance spectroscopy* **59**, 271-292, doi:10.1016/j.pnmrs.2011.02.002 (2011).
38 Widmalm, G. A perspective on the primary and three-dimensional structures of carbohydrates. *Carbohydrate research* **378**, 123-132, doi:10.1016/j.carres.2013.02.005 (2013).
39 Bernlind, C., Oscarson, S. & Widmalm, G. Synthesis, NMR, and conformational studies of methyl α-d-mannopyranoside 2-, 3-, 4-, and 6-monophosphates. *Carbohydrate research* **263**, 173-180 (1994).
40 Marino, J. P. *et al.* Three-Dimensional Triple-Resonance 1H, 13C, 31P Experiment: Sequential Through-Bond Correlation of Ribose Protons and Intervening Phosphorus along the RNA Oligonucleotide Backbone. *J. Am. Chem. Soc.* **116**, 6472-6473 (1994).
41 Endl, J., Seidl, H. P., Fiedler, F. & Schleifer, K. H. Chemical composition and structure of cell wall teichoic acids of staphylococci. *Archives of microbiology* **135**, 215-223 (1983).
42 Fischer, W., Behr, T., Hartmann, R., Peter-Katalinic, J. & Egge, H. Teichoic acid and lipoteichoic acid of Streptococcus pneumoniae possess identical chain structures. A reinvestigation of teichoid acid (C polysaccharide). *Eur J Biochem* **215**, 851-857 (1993).
43 Potekhina, N. V., Tul'skaya, E. M., Naumova, I. B., Shashkov, A. S. & Evtushenko, L. I. Erythritolteichoic acid in the cell wall of Glycomyces tenuis VKM Ac-1250. *Eur J Biochem* **218**, 371-375 (1993).
44 Salton, M. R. & Horne, R. W. Studies of the bacterial cell wall. II. Methods of preparation and some properties of cell walls. *Biochim Biophys Acta* **7**, 177-197 (1951).
45 Michon, F., Brisson, J. R., Dell, A., Kasper, D. L. & Jennings, H. J. Multiantennary group-specific polysaccharide of group B Streptococcus. *Biochemistry* **27**, 5341-5351 (1988).
46 Pritchard, D. G., Gray, B. M. & Dillon, H. C., Jr. Characterization of the group-specific polysaccharide of group B Streptococcus. *Arch Biochem Biophys* **235**, 385-392 (1984).
47 Janczura, E., Perkins, H. R. & Rogers, H. J. Teichuronic acid: a mucopolysaccharide present in wall preparations from vegetative cells of Bacillus subtilis. *Biochem J* **80**, 82-93 (1961).
48 Soldo, B., Lazarevic, V., Pagni, M. & Karamata, D. Teichuronic acid operon of Bacillus subtilis 168. *Mol Microbiol* **31**, 795-805 (1999).
49 Choudhury, B. *et al.* The structure of the major cell wall polysaccharide of Bacillus anthracis is species-specific. *J Biol Chem* **281**, 27932-27941, doi:10.1074/jbc.M605768200 (2006).
50 Hay, J. B., Wicken, A. J. & Baddiley, J. The location of intracellular teichoic acids. *Biochim Biophys Acta* **71**, 188-190 (1963).
51 Kelemen, M. V. & Baddiley, J. Structure of the intracellular glycerol teichoic acid from Lactobacillus casei A.T.C.C. 7469. *Biochem J* **80**, 246-254 (1961).
52 Shockman, G. D. & Slade, H. D. The Cellular Location of the Streptococcal Group D Antigen. *Journal of general microbiology* **37**, 297-305, doi:10.1099/00221287-37-3-297 (1964).
53 Toon, P., Brown, P. E. & Baddiley, J. The lipid-teichoic acid complex in the cytoplasmic membrane of Streptococcus faecalis N.C.I.B. 8191. *Biochem J* **127**, 399-409 (1972).
54 Wicken, A. J. & Knox, K. W. Studies on the group F antigen of lactobacilli: isolation of a teichoic acid-lipid complex from Lactobacillus fermenti NCTC 6991. *Journal of general microbiology* **60**, 293-301, doi:10.1099/00221287-60-3-293 (1970).

55 Biswas, R. *et al.* Proton-binding capacity of Staphylococcus aureus wall teichoic acid and its role in controlling autolysin activity. *PLoS One* **7**, e41415, doi:10.1371/journal.pone.0041415 (2012).
56 Hughes, A. H., Hancock, I. C. & Baddiley, J. The function of teichoic acids in cation control in bacterial membranes. *Biochem J* **132**, 83-93 (1973).
57 Lambert, P. A., Hancock, I. C. & Baddiley, J. The interaction of magnesium ions with teichoic acid. *Biochem J* **149**, 519-524 (1975).
58 Marquis, R. E., Mayzel, K. & Carstensen, E. L. Cation exchange in cell walls of gram-positive bacteria. *Canadian journal of microbiology* **22**, 975-982 (1976).
59 Neuhaus, F. C. & Baddiley, J. A continuum of anionic charge: structures and functions of D-alanyl-teichoic acids in gram-positive bacteria. *Microbiol Mol Biol Rev* **67**, 686-723 (2003).
60 Rose, R. K., Hogg, S. D. & Shellis, R. P. A quantitative study of calcium binding by isolated streptococcal cell walls and lipoteichoic acid: comparison with whole cells. *Journal of dental research* **73**, 1742-1747, doi:10.1177/00220345940730111001 (1994).
61 Thomas, K. J., 3rd & Rice, C. V. Revised model of calcium and magnesium binding to the bacterial cell wall. *Biometals : an international journal on the role of metal ions in biology, biochemistry, and medicine* **27**, 1361-1370, doi:10.1007/s10534-014-9797-5 (2014).
62 Thomas, K. J., 3rd & Rice, C. V. Equilibrium binding behavior of magnesium to wall teichoic acid. *Biochim Biophys Acta* **1848**, 1981-1987, doi:10.1016/j.bbamem.2015.05.003 (2015).
63 Caliot, E. *et al.* Role of the Group B antigen of Streptococcus agalactiae: a peptidoglycan-anchored polysaccharide involved in cell wall biogenesis. *PLoS Pathog* **8**, e1002756, doi:10.1371/journal.ppat.1002756 (2012).
64 Mc, C. M. & Lancefield, R. C. Variation in the group-specific carbohydrate of group A streptococci. I. Immunochemical studies on the carbohydrates of variant strains. *J Exp Med* **102**, 11-28 (1955).
65 Pritchard, D. G., Gregory, R. L., Michalek, S. M. & McGhee, J. R. Characterization of the serotype e polysaccharide antigen of Streptococcus mutans. *Molecular immunology* **23**, 141-145 (1986).
66 Pritchard, D. G., Michalek, S. M., McGhee, J. R. & Furner, R. L. Structure of the serotype f polysaccharide antigen of Streptococcus mutans. *Carbohydrate research* **166**, 123-131 (1987).
67 Heymann, H., Manniello, J. M. & Barkulis, S. S. Structure of streptococcal cell walls. V. Phosphate esters in the walls of group A Streptococcus pyogenes. *Biochem Biophys Res Commun* **26**, 486-491 (1967).
68 Pazur, J. H., Cepure, A., Kane, J. A. & Karakawa, W. W. Glycans from streptococcal cell walls: glycosyl-phosphoryl moieties as immunodominant groups in heteroglycans from group D and group L streptococci. *Biochem Biophys Res Commun* **43**, 1421-1428 (1971).
69 Prakobphol, A., Linzer, R. & Genco, R. J. Purification and characterization of a rhamnose-containing cell wall antigen of Streptococcus mutans B13 (serotype d). *Infect Immun* **27**, 150-157 (1980).
70 Czabanska, A., Holst, O. & Duda, K. A. Chemical structures of the secondary cell wall polymers (SCWPs) isolated from bovine mastitis Streptococcus uberis. *Carbohydrate research* **377**, 58-62, doi:10.1016/j.carres.2013.05.015 (2013).
71 Neiwert, O., Holst, O. & Duda, K. A. Structural investigation of rhamnose-rich polysaccharides from Streptococcus dysgalactiae bovine mastitis isolate. *Carbohydrate research* **389**, 192-195, doi:10.1016/j.carres.2013.12.018 (2014).
72 Lequette, Y., Lanfroy, E., Cogez, V., Bohin, J. P. & Lacroix, J. M. Biosynthesis of osmoregulated periplasmic glucans in Escherichia coli: the membrane-bound and the soluble periplasmic phosphoglycerol transferases are encoded by the same gene. *Microbiology* **154**, 476-483, doi:10.1099/mic.0.2007/013169-0 (2008).

73 Karatsa-Dodgson, M., Wormann, M. E. & Grundling, A. In vitro analysis of the Staphylococcus aureus lipoteichoic acid synthase enzyme using fluorescently labeled lipids. *J Bacteriol* **192**, 5341-5349, doi:10.1128/JB.00453-10 (2010).
74 Vinogradov, E. *et al.* Determination of the cell wall polysaccharide and teichoic acid structures from Lactococcus lactis IL1403. *Carbohydrate research* **462**, 39-44, doi:10.1016/j.carres.2018.04.002 (2018).
75 Vinogradov, E. *et al.* Structural studies of the cell wall polysaccharide from Lactococcus lactis UC509.9. *Carbohydrate research* **461**, 25-31, doi:10.1016/j.carres.2018.03.011 (2018).
76 Geno, K. A. *et al.* Pneumococcal Capsules and Their Types: Past, Present, and Future. *Clin Microbiol Rev* **28**, 871-899, doi:10.1128/CMR.00024-15 (2015).
77 Rundlof, T. & Widmalm, G. A method for determination of the absolute configuration of chiral glycerol residues in natural products using TEMPO oxidation and characterization of the glyceric acids formed. *Analytical biochemistry* **243**, 228-233, doi:10.1006/abio.1996.0510 (1996).
78 Calix, J. J., Nahm, M. H. & Zartler, E. R. Elucidation of structural and antigenic properties of pneumococcal serotype 11A, 11B, 11C, and 11F polysaccharide capsules. *J Bacteriol* **193**, 5271-5278, doi:10.1128/JB.05034-11 (2011).
79 Bertsche, U. *et al.* Correlation of daptomycin resistance in a clinical Staphylococcus aureus strain with increased cell wall teichoic acid production and D-alanylation. *Antimicrob Agents Chemother* **55**, 3922-3928, doi:10.1128/AAC.01226-10 (2011).
80 Hunt, C. L., Nauseef, W. M. & Weiss, J. P. Effect of D-alanylation of (lipo)teichoic acids of Staphylococcus aureus on host secretory phospholipase A2 action before and after phagocytosis by human neutrophils. *J Immunol* **176**, 4987-4994 (2006).
81 Peschel, A. How do bacteria resist human antimicrobial peptides? *Trends Microbiol* **10**, 179-186 (2002).
82 Peschel, A. *et al.* Inactivation of the dlt operon in Staphylococcus aureus confers sensitivity to defensins, protegrins, and other antimicrobial peptides. *J Biol Chem* **274**, 8405-8410 (1999).
83 Peschel, A., Vuong, C., Otto, M. & Gotz, F. The D-alanine residues of Staphylococcus aureus teichoic acids alter the susceptibility to vancomycin and the activity of autolytic enzymes. *Antimicrob Agents Chemother* **44**, 2845-2847 (2000).
84 Yang, S. J. *et al.* Enhanced expression of dltABCD is associated with the development of daptomycin nonsusceptibility in a clinical endocarditis isolate of Staphylococcus aureus. *J Infect Dis* **200**, 1916-1920, doi:10.1086/648473 (2009).
85 Archibald, A. R., Baddiley, J. & Heptinstall, S. The alanine ester content and magnesium binding capacity of walls of Staphylococcus aureus H grown at different pH values. *Biochim Biophys Acta* **291**, 629-634 (1973).
86 Falagas, M. E., Rafailidis, P. I. & Matthaiou, D. K. Resistance to polymyxins: Mechanisms, frequency and treatment options. *Drug resistance updates : reviews and commentaries in antimicrobial and anticancer chemotherapy* **13**, 132-138, doi:10.1016/j.drup.2010.05.002 (2010).
87 Djoko, K. Y., Ong, C. L., Walker, M. J. & McEwan, A. G. The Role of Copper and Zinc Toxicity in Innate Immune Defense against Bacterial Pathogens. *J Biol Chem* **290**, 18954-18961, doi:10.1074/jbc.R115.647099 (2015).
88 McDevitt, C. A. *et al.* A molecular mechanism for bacterial susceptibility to zinc. *PLoS Pathog* **7**, e1002357, doi:10.1371/journal.ppat.1002357 (2011).
89 Buckland, A. G. & Wilton, D. C. Inhibition of secreted phospholipases A2 by annexin V. Competition for anionic phospholipid interfaces allows an assessment of the relative interfacial affinities of secreted phospholipases A2. *Biochim Biophys Acta* **1391**, 367-376 (1998).

90 Hsu, Y. H., Dumlao, D. S., Cao, J. & Dennis, E. A. Assessing phospholipase A2 activity toward cardiolipin by mass spectrometry. *PLoS One* **8**, e59267, doi:10.1371/journal.pone.0059267 (2013).
91 Koprivnjak, T., Peschel, A., Gelb, M. H., Liang, N. S. & Weiss, J. P. Role of charge properties of bacterial envelope in bactericidal action of human group IIA phospholipase A2 against Staphylococcus aureus. *J Biol Chem* **277**, 47636-47644, doi:10.1074/jbc.M205104200 (2002).
92 Johnson, M. A. & Pinto, B. M. NMR spectroscopic and molecular modeling studies of protein-carbohydrate and protein-peptide interactions. *Carbohydrate research* **339**, 907-928, doi:10.1016/j.carres.2003.12.028 (2004).
93 Carapetis, J. R., Steer, A. C., Mulholland, E. K. & Weber, M. The global burden of group A streptococcal diseases. *Lancet Infect Dis* **5**, 685-694, doi:10.1016/S1473-3099(05)70267-X (2005).
94 Adderson, E. E., Shikhman, A. R., Ward, K. E. & Cunningham, M. W. Molecular analysis of polyreactive monoclonal antibodies from rheumatic carditis: human anti-N-acetylglucosamine/anti-myosin antibody V region genes. *J Immunol* **161**, 2020-2031 (1998).
95 Goldstein, I., Rebeyrotte, P., Parlebas, J. & Halpern, B. Isolation from heart valves of glycopeptides which share immunological properties with Streptococcus haemolyticus group A polysaccharides. *Nature* **219**, 866-868 (1968).
96 Ayoub, E. M. & Dudding, B. A. Streptococcal group A carbohydrate antibody in rheumatic and nonrheumatic bacterial endocarditis. *The Journal of laboratory and clinical medicine* **76**, 322-332 (1970).
97 Kirvan, C. A., Swedo, S. E., Heuser, J. S. & Cunningham, M. W. Mimicry and autoantibody-mediated neuronal cell signaling in Sydenham chorea. *Nature medicine* **9**, 914-920, doi:10.1038/nm892 (2003).
98 Shulman, S. T. *et al.* Group A streptococcal pharyngitis serotype surveillance in North America, 2000-2002. *Clin Infect Dis* **39**, 325-332, doi:10.1086/421949 (2004).
99 Sumby, P. *et al.* Evolutionary origin and emergence of a highly successful clone of serotype M1 group a Streptococcus involved multiple horizontal gene transfer events. *J Infect Dis* **192**, 771-782 (2005).
100 Koga, T., Asakawa, H., Okahashi, N. & Takahashi, I. Effect of subculturing on expression of a cell-surface protein antigen by Streptococcus mutans. *Journal of general microbiology* **135**, 3199-3207, doi:10.1099/00221287-135-12-3199 (1989).
101 Moore, G. E., Gerner, R. E. & Franklin, H. A. Culture of normal human leukocytes. *Jama* **199**, 519-524 (1967).
102 van de Rijn, I. & Kessler, R. E. Growth characteristics of group A streptococci in a new chemically defined medium. *Infect Immun* **27**, 444-448 (1980).
103 Hoff, J. S., DeWald, M., Moseley, S. L., Collins, C. M. & Voyich, J. M. SpyA, a C3-like ADP-ribosyltransferase, contributes to virulence in a mouse subcutaneous model of Streptococcus pyogenes infection. *Infection and immunity* **79**, 2404-2411, doi:10.1128/IAI.01191-10 (2011).
104 Caparon, M. G. & Scott, J. R. Genetic manipulation of pathogenic streptococci. *Methods Enzymol* **204**, 556-586 (1991).
105 Horton, R. M., Hunt, H. D., Ho, S. N., Pullen, J. K. & Pease, L. R. Engineering hybrid genes without the use of restriction enzymes: gene splicing by overlap extension. *Gene* **77**, 61-68 (1989).
106 Trevino, J., Liu, Z., Cao, T. N., Ramirez-Pena, E. & Sumby, P. RivR is a negative regulator of virulence factor expression in group A Streptococcus. *Infection and immunity* **81**, 364-372, doi:10.1128/IAI.00703-12 (2013).
107 Kabsch, W. Xds. *Acta crystallographica. Section D, Biological crystallography* **66**, 125-132, doi:10.1107/S0907444909047337 (2010).

108 Grosse-Kunstleve, R. W. & Adams, P. D. Substructure search procedures for macromolecular structures. *Acta crystallographica. Section D, Biological crystallography* **59**, 1966-1973 (2003).
109 McCoy, A. J., Storoni, L. C. & Read, R. J. Simple algorithm for a maximum-likelihood SAD function. *Acta crystallographica. Section D, Biological crystallography* **60**, 1220-1228, doi:10.1107/S0907444904009990 (2004).
110 Terwilliger, T. C. *et al.* Decision-making in structure solution using Bayesian estimates of map quality: the PHENIX AutoSol wizard. *Acta crystallographica. Section D, Biological crystallography* **65**, 582-601, doi:10.1107/S0907444909012098 (2009).
111 Emsley, P., Lohkamp, B., Scott, W. G. & Cowtan, K. Features and development of Coot. *Acta crystallographica. Section D, Biological crystallography* **66**, 486-501, doi:10.1107/S0907444910007493 (2010).
112 Afonine, P. V. *et al.* Towards automated crystallographic structure refinement with phenix.refine. *Acta crystallographica. Section D, Biological crystallography* **68**, 352-367, doi:10.1107/S0907444912001308 (2012).
113 McCoy, A. J. *et al.* Phaser crystallographic software. *Journal of applied crystallography* **40**, 658-674, doi:10.1107/S0021889807021206 (2007).
114 Adams, P. D. *et al.* PHENIX: a comprehensive Python-based system for macromolecular structure solution. *Acta crystallographica. Section D, Biological crystallography* **66**, 213-221, doi:10.1107/S0907444909052925 (2010).
115 Chen, V. B. *et al.* MolProbity: all-atom structure validation for macromolecular crystallography. *Acta crystallographica. Section D, Biological crystallography* **66**, 12-21, doi:10.1107/S0907444909042073 (2010).
116 Gore, S. *et al.* Validation of Structures in the Protein Data Bank. *Structure* **25**, 1916-1927, doi:10.1016/j.str.2017.10.009 (2017).
117 Schrodinger, LLC. *The PyMOL Molecular Graphics System, Version 1.8.0.3* (2010).
118 Bui, N. K. *et al.* Isolation and analysis of cell wall components from Streptococcus pneumoniae. *Analytical biochemistry* **421**, 657-666, doi:10.1016/j.ab.2011.11.026 (2012).
119 Santander, J. *et al.* Mechanisms of intrinsic resistance to antimicrobial peptides of Edwardsiella ictaluri and its influence on fish gut inflammation and virulence. *Microbiology* **159**, 1471-1486, doi:10.1099/mic.0.066639-0 (2013).
120 Ghomashchi, F. *et al.* Preparation of the Full Set of Recombinant Mouse- and Human-Secreted Phospholipases A2. *Methods Enzymol* **583**, 35-69, doi:10.1016/bs.mie.2016.10.034 (2017).
121 Le Breton, Y. & McIver, K. S. Genetic manipulation of Streptococcus pyogenes (the Group A Streptococcus, GAS). *Current protocols in microbiology* **30**, Unit 9D 3, doi:10.1002/9780471729259.mc09d03s30 (2013).
122 Wagner, R. & Berger, S. Gradient-Selected NOESY-A Fourfold Reduction of the Measurement Time for the NOESY Experiment. *Journal of magnetic resonance. Series A* **123**, 119-121 (1996).
123 Willker, W., Leibfritz, D., Kerssebaum, R. & Bermel, W. Gradient selection in inverse heteronuclear correlation spectroscopy. *Magnetic Resonance in Chemistry* **31**, 287-292 (1993).
124 Kellogg, G. W. Proton-detected hetero-TOCSY experiments with application to nucleic acids. *Journal of Magnetic Resonance* **98**, 176-182 (1992).
125 Tsirigos, K. D., Peters, C., Shu, N., Kall, L. & Elofsson, A. The TOPCONS web server for consensus prediction of membrane protein topology and signal peptides. *Nucleic Acids Res* **43**, W401-407, doi:10.1093/nar/gkv485 (2015).
126 Soding, J., Biegert, A. & Lupas, A. N. The HHpred interactive server for protein homology detection and structure prediction. *Nucleic Acids Res* **33**, W244-248, doi:10.1093/nar/gki408 (2005).

127 Edgar, R. C. MUSCLE: multiple sequence alignment with high accuracy and high throughput. *Nucleic Acids Res* **32**, 1792-1797, doi:10.1093/nar/gkh340 (2004).
128 Tamura, K., Stecher, G., Peterson, D., Filipski, A. & Kumar, S. MEGA6: Molecular Evolutionary Genetics Analysis version 6.0. *Molecular biology and evolution* **30**, 2725-2729, doi:10.1093/molbev/mst197 (2013).